

NASA TECHNICAL  
MEMORANDUM

NASA TM X-53677

November 28, 1967

NASA TM X-53677

SURVEY AND COMPARATIVE ANALYSIS OF  
CURRENT GEOPHYSICAL MODELS

By Jesco von Puttkamer  
Aero-Astroynamics Laboratory

FACILITY FORM 602	N 68-17043 (ACCESSION NUMBER)	(THRU)
	70 (PAGES)	1 (CODE)
	TMX-53677 (NASA CR OR TMX OR AD NUMBER)	13 (CATEGORY)

NASA

*George C. Marshall  
Space Flight Center,  
Huntsville, Alabama*

TECHNICAL MEMORANDUM X-53677

SURVEY AND COMPARATIVE ANALYSIS OF CURRENT GEOPHYSICAL MODELS

By

Jesco von Puttkamer

George C. Marshall Space Flight Center

Huntsville, Alabama

ABSTRACT

By using currently accepted constants of geodesy, notably several different sets of oblateness coefficients, seven models of the geometry of the earth and its gravitational field, including the currently valid NASA Standard Model, are numerically derived and compared with each other and with a newly developed geoid based on recent measurements of the secular and periodic perturbations of artificial satellite orbits.

NASA - GEORGE C. MARSHALL SPACE FLIGHT CENTER

---

Technical Memorandum X-53677

---

November 28, 1967

SURVEY AND COMPARATIVE ANALYSIS OF CURRENT GEOPHYSICAL MODELS

By

Jesco von Puttkamer

TECHNICAL AND SCIENTIFIC STAFF  
AERO-ASTRODYNAMICS LABORATORY  
RESEARCH AND DEVELOPMENT OPERATIONS

## TABLE OF CONTENTS

	<u>Page</u>
I. INTRODUCTION.....	1
II. GENERAL BACKGROUND AND DISCUSSION OF THE PROBLEM.....	3
A. The Potential Function of the Earth.....	3
B. The Spherical Harmonics.....	5
C. The Harmonics Coefficients.....	7
D. The Theory of Clairaut.....	9
E. The Geoid.....	14
F. Determination of the Harmonics Coefficients.....	15
G. Krause's Theory of the Geoid Surface.....	17
III. Analysis of Models.....	21
A. Model 1 ( $J_2$ -Only).....	21
B. Model 2 (NASA Standard).....	25
C. Model 3 (New $J_2$ , $J_3$ , $J_4$ ).....	31
D. Higher-Order Bodies with Equator Symmetry.....	34
1. Model 4a (Triaxial Ellipsoid).....	34
2. Model 4b (Symmetrical Geoid).....	39
E. "Best" Geoid Bodies.....	40
1. Model 5a ("Best" Geoid with Sectorial Term).....	40
2. Model 5b ("Best" Geoid without Sectorial Term)...	46
IV. COMPARISON OF MODELS.....	46
V. CONCLUSIONS.....	54
APPENDIX A. COMPUTATION OF LEGENDRE POLYNOMIALS.....	57
APPENDIX B. ALTERNATE EXPRESSION FOR THE GRAVITY ACCELERATION.	59

LIST OF ILLUSTRATIONS

<u>Figure</u>	<u>Title</u>	<u>Page</u>
1	First Sectorial Harmonic (due to $J_{2,2}$ ) at Equator....	8
2	Second Spherical Harmonics Terms in Earth Geoid.....	10
3	Third and Fourth Order Spherical Harmonics Terms in Earth Geoid.....	11
4	Fifth and Sixth Order Spherical Harmonics Terms in Earth Geoid.....	12
5	Height of $J_2$ -Spheroid (Model 1) over Reference Ellipsoid of Flattening 1/298.222 (Model 3).....	26
6	Heights of Models 1, 2 and 3 (Spheroids) over "Best" Geoid without Sectorial Term.....	47
7	Heights of Model 2 Spheroid, and of "Best" Geoid Without Sectorial Term, over Standard Ellipsoid (1/298.3).....	48
8	Heights of Model 3 Spheroid, and of "Best" Geoid without Sectorial Term, over Ellipsoid of Flattening 1/298.222.....	50
9	Heights of "Best" Geoid (Model 5) over Triaxial Ellipsoid of Flattening 1/298.184, Along Prime Meridian.....	51
10	Heights of "Best" Geoid (Model 5) over Triaxial Ellipsoid of Flattening 1/298.184, Along Prime Meridian.....	52
11	Deviations of Gravities of Models 1, 2, 3 and 4 from Gravity of "Best" Geoid (Model 5), Along Prime Meridian.....	53

## DEFINITION OF SYMBOLS

<u>Symbol</u>	<u>Definition</u>
$A_n$	coefficients in the series expansion for the geoid radius
$A_{2,2}$	coefficient of the sectorial harmonic in the geoid expansion
$B_2$	coefficient in the series expansion of the geoid radius
$C_{n,m}$	numerical coefficients in the geopotential function
$f$	flattening or oblateness
$f_e$	ellipticity (or flattening) of the equator
$g_e$	gravity at the equator
$\bar{g}_e$	mean equatorial gravity
$GM_{\oplus}$	gravitational parameter of the earth (= $\mu$ )
$J_n$	coefficients of zonal harmonics in geopotential
$J_{n,m}$	coefficients of tesseral harmonics in geopotential
$J_{n,n}$	coefficients of sectorial harmonics in geopotential
$\left. \begin{array}{l} J \\ H \\ D \end{array} \right\}$	oblateness coefficients (older notation)
$m$	centrifugal factor at the equator <u>also:</u> index in series notation
$P_n^m(\sin \vartheta)$	associated Legendre polynomials of degree $n$ and order $m$
$P_n(\sin \vartheta)$	Legendre polynomials of $n$ th degree
$R_e$	equatorial radius of the earth
$\bar{R}_e$	mean equatorial radius of the earth
$R_p$	polar radius of the earth

## DEFINITION OF SYMBOLS (Continued)

<u>Symbol</u>	<u>Definition</u>
$R_{pN}$	north polar radius of the earth
$R_{pS}$	south polar radius of the earth
$R_{e0}$	longest equatorial radius of the earth
$R_{e1}$	shortest equatorial radius of the earth
$r$	radial distance from the center of the earth
$U$	potential function
$\lambda$	geographic longitude, positive east of Greenwich
$\lambda_0$	longitude of the longest equatorial radius (semi-major axis)
$\mu$	gravitational parameter of the earth
$\sigma$	factor in equatorial gravity acceleration equation
$\varnothing$	geocentric latitude
$\chi$	factor defined by equation (22)
$\omega$	angular velocity of the earth's rotation
$\tilde{\omega}_e$	centrifugal factor at the equator
$\psi$	perturbation parameter in potential function

## TECHNICAL MEMORANDUM X-53677

### SURVEY AND COMPARATIVE ANALYSIS OF CURRENT GEOPHYSICAL MODELS

#### SUMMARY

By using currently accepted constants of geodesy, especially several different sets of oblateness coefficients, seven models of the geometry of the earth and its gravitational field are numerically derived and compared with each other and with a newly developed geopotential based on recent measurements of the secular and periodic perturbations of artificial satellite orbits.

Conclusions are drawn which show, among other things, that the currently used NASA Standard Model deviates significantly from the "best" geoid, and that there are better analytical, as well as numerical, models by which improved approximation can be achieved.

Also, it is shown that improvements in the numerical values of the used oblateness coefficients, rather than in their number, appear to have little influence on the values of the gravity, but that they affect the geometries significantly. Increasing the number of zonal harmonics coefficients, however, can lead to considerable improvements in the gravity model, at least in the range studied (up to and including  $J_{14}$ ).

#### I. INTRODUCTION

In the past a number of theories of varying complexity have been developed to describe the figure and the gravitation field of the earth for use in geodetic, astrodynamic, and astronomical calculations.

In scrutinizing these theories, a number of discrepancies are manifest which appear to be caused by two factors; i.e., (1) inherent inconsistencies in the development of some of the theories, and (2) differences in gravitational and geometrical parameters used by their authors.

With regard to the first consideration, while the earth's gravitational potential (i.e., the potential energy of the earth in relation to the position relative to the earth) is commonly expressed by the potential function as a series of spherical harmonics, as adopted by the International Astronomical Union (IAU)<sup>1\*</sup>, the shape of the earth

---

\* Superscripts in text indicate references at end of report.



introduced in the geopotential at the earth's surface with the simultaneous assumption that the potential along the surface of the geoid is constant, is that of an ellipsoid which approximates the actual geoid. The flattening of the ellipsoid is usually determined approximately by the astrogeodetic methods of geometrical geodesy (sometimes also by the less accurate techniques of gravimetry), using variants of Clairaut's theorem. However, even if higher-order extensions of the latter are used, they remain only approximations, which become increasingly inaccurate for increasing deviation of the geopotential from that of a regular ellipsoid.

The second consideration refers to the fact that, with our increasing knowledge of our globe and its gravity anomalies, the descriptive geographical parameters are subject to change, particularly the number and values of the oblateness coefficients, but also -- to a lesser degree -- the gravitational parameter  $GM_{\oplus}$ , and the geometrical parameters flattening  $f$ , and mean equatorial radius  $\bar{R}_e$ . Urgently needed standardization of the principal parameters was accomplished by NASA in 1963, but new and additional data have been determined continuously ever since and are being determined from an ever-increasing population of artificial satellites in precision-tracked (Baker-Nunn) orbits of all inclinations.

To relate these new observations to the geoid without having to accept the inconsistencies of the second- and third-order Clairaut extensions, a new theory was developed recently at MSFC by H. Krause<sup>13,14</sup>, which further increased the bulk of existing geographic parameters and models.

It is the objective of the following analysis to define and to compare seven different geographic models, one of which is the current (but outdated) NASA Standard. These models are based on four different sets of oblateness coefficients, all of which are applicable to present practical work, and also on the fact that for each set of oblateness conditions two body geometries can be defined; i.e., a spheroid composed of superimposed spherical harmonics and a regular ellipsoid approximating this spheroid.

In the first part of the analysis, the general background and the nature of the problem is considered in some detail, followed by the derivation and description of the geophysical theories. In the third part, the models are compared with each other. A number of salient conclusions, forming the fourth part, can then be drawn.

## II. GENERAL BACKGROUND AND DISCUSSION OF THE PROBLEM

### A. The Potential Function of the Earth

In the study of geocentric motion such as that encountered on rocket trajectories and satellite orbits, among the most important constants necessary for describing the environment are those pertaining to the gravity field acting on the moving body, and to the shape or figure of the gravitating body, the earth.

Theories attempting to describe the earth's gravity field are, by necessity, fundamentally based on Newton's Universal Law of Gravitation, which is rigorously accurate for a central force field as produced by a perfectly homogeneous and perfectly spherical body. The gravitational potential of such a Newtonian force field is

$$U = - \frac{\mu}{r} . \quad (1)$$

The potential function of the earth  $U_{\oplus}$ , or the geopotential, is defined as the integral of the gravity forces over the entire field, which are the resultant of the gravitational forces due to Newtonian attraction and the centrifugal force due to the rotation of the earth and its atmosphere. Thus, the geopotential is the sum of the potential of the gravitational field and the potential of the centrifugal force.

$$U_{\oplus} = - \frac{\mu}{r} (1 + \psi) + \frac{1}{2} \omega^2 r^2 \cos^2 \vartheta . \quad (2)$$

If the rotational term is omitted, equation (2) expresses the gravitational potential which is appropriate to inertial coordinates, as useful for exo-atmospheric (free-flight) flight phases. For geodesy, as well as for all other applications requiring a rotating earth coordinate system, the term is retained.

In equation (2), the modifier  $\psi$  accounts for the fact that, contrary to the basic assumptions of the Newtonian potential, the earth's internal mass distribution is not entirely homogeneous and its shape is not spherical, but oblate. Also, its surface is covered with irregularities, such as continental highlands, depressions, mountain ranges, ocean deeps, valleys, etc., which give rise to gravitational anomalies and require an additive perturbative term to complete the geopotential.

Since the potential function of the earth is a solution of the Laplace equation ( $\nabla^2 U_{\oplus} = 0$ ), it is a harmonic function and can be represented analytically as the sum of a series of two-dimensional (spherical) harmonics in a manner similar to the one-dimensional Fourier series as representation of a nonanalytical function on a circle. The coefficients of the terms of this infinite (converging) series are polynomials of the general Legendre type, while the terms themselves are the so-called surface harmonics, the introduction of which is due to Legendre and Laplace. If the spherical harmonic is a function of two variables, such as latitude and longitude (rather than only one, the latitude), it involves the so-called Associated Legendre Polynomials.

The acceleration of gravity  $g$  of the earth is defined as  $\nabla U$  and can therefore also be expressed in spherical harmonics.

The perturbative parameter  $\psi$  of the gravitational potential in equation (2) can be expanded, as described, in an infinite series of spherical harmonics.

$$\psi = \sum_{n=1}^{\infty} \sum_{m=0}^n \left( \frac{\bar{R}_e}{r} \right)^n P_n^m(\sin \vartheta) \left[ C_{n,m} \cos m\lambda + S_{n,m} \sin m\lambda \right], \quad (3)$$

where  $r$  is the distance from the center of the earth,  $\bar{R}_e$  is the earth's mean equatorial radius,  $\vartheta$  is the latitude,  $\lambda$  is the longitude,  $C_{n,m}$  and  $S_{n,m}$  are numerical coefficients, and the  $P_n^m$  are the associated Legendre polynomials. Introducing equation (3) in equation (2), one obtains the general formula for the earth potential, as recommended by the IAU (1962)<sup>3,1</sup>.

$$U = \frac{\mu}{r} \left[ 1 + \sum_{n=1}^{\infty} \sum_{m=0}^n \left( \frac{\bar{R}_e}{r} \right)^n \cdot P_n^m(\sin \varphi) (C_{n,m} \cos m\lambda + S_{n,m} \sin m\lambda) \right] + \frac{1}{2} \omega^2 r^2 \cos^2 \varphi. \quad (4)$$

### B. The Spherical Harmonics

It is seen that the second (aspherical) part of equation (4) consists of an infinite series of harmonics which -- in a rigorous sense -- describes the perturbative potential accurately only if an infinite number of terms are considered. Taking the terms by families according to the indices, it is furthermore seen that for the first existing family, where  $m = 0$ ,  $1 < n < \infty$ , the equation reduces to

$$U_{m=0} = \frac{\mu}{r} \left[ 1 + \sum_{n=1}^{\infty} \left( \frac{\bar{R}_e}{r} \right)^n \cdot P_n(\sin \varphi) \cdot C_n \right]. \quad (5)$$

for the purely gravitational potential.

In this special case,  $P_n(\sin \varphi)$  are the (simple) Legendre polynomials of argument  $\sin \varphi$ , usually referred to as "zonal" harmonics. Obviously, the potential  $U_{m=0}$  is independent of the longitude  $\lambda$ ; hence, it is constant along (latitude) parallels. This means that the undulations of the harmonics on the sphere are zero along parallels and become alternately positive and negative between these  $n$  parallels in a distance  $\pi$ . Thus, equation (5) refers to an axially symmetric earth which is fluted along the parallels and where the symmetry axis is the rotational axis through the poles.

As an alternate for  $C_{n,0}$ , it has been recommended by the IAU<sup>1</sup> to use

$$J_n = -C_{n,0}. \quad (6)$$

Thus, for the body-of-revolution case, the purely gravitational potential becomes

$$U_{m=0} = \frac{\mu}{r} \left[ 1 - \sum_{n=1}^{\infty} J_n \cdot \left( \frac{\bar{R}_e}{r} \right)^n \cdot P_n(\sin \varphi) \right]. \quad (7)$$

The true figure of the earth does not exactly exhibit rotational symmetry, as assumed by setting  $m = 0$  in equation (4). The principal axes of inertia of the true earth do not exactly coincide with the rotational axis system. Thus, the angular momentum of the earth is not pointing exactly in the same direction as the angular velocity. Consequently, products of inertia do exist, which are represented by higher harmonics. By letting  $m$  assume integral values from 1 to  $n$ , terms are added to the second part of equation (5), which include the longitude  $\lambda$  as a second variable. Consequently, the associated Legendre polynomials  $P_n^m(\sin \varphi)$  are also required, as well as coefficients  $J_{n,m}$ . These terms are referred to as tesseral harmonics, with the exception of the two terms in equation (4) resulting from letting  $m = n$ , so that

$$C_{n,n} P_n^n \cos n\lambda \quad \text{and} \quad S_{n,n} P_n^n \sin n\lambda$$

appear. These two terms are called "sectorial" harmonics.

The tesseral harmonics ( $0 < m < n$ ) have zeros both along meridians and along parallels; thus, the undulations represented by them become zero on the reference spheroid simultaneously on a number of meridians and parallels. They undulate in the form of a network across the spheroid similar to a chessboard composed of fields that are alternately positive and negative. Thus, for example, the spherical harmonic represented by the function  $P_6^4$  (with the coefficient  $J_{6,4}^*$ ) forms a network of five

---

\* The notation used commonly in the literature for the tesseral and sectorial  $J$ -coefficients is  $J_{nm}$ . Thus, the first sectorial harmonics coefficient would be  $J_{22}$ , the first tesseral coefficient  $J_{12}$ , etc. While this practice represented an ambiguity in notation, with respect to the zonal harmonics, no great confusion could be caused as long as the zonal harmonics used in practical work did not exceed the tenth order. With present analyses of the higher zonal harmonics already going to  $n = 21$ ,  $m = 0$ ,<sup>4</sup> however, notation of the mentioned type would easily confuse tesseral with zonal harmonics. Thus, the zonal  $J_{14}$  could easily be interpreted as the tesseral  $n = 1, m = 4$ . Since powers of  $J_n$  are sometimes encountered, the old practice of writing  $J_n^m$  is also not desirable. Consequently, it is suggested that tesseral and sectorial coefficients are indexed with a dividing comma, i.e.,  $J_{n,m}$ , while the zonal notation  $J_n$  be retained. The notation  $P_n^m$  for the associated Legendre polynomials should also remain unchanged.

meridians (four zeros in  $180^\circ$ ) and  $(6 - 4) = 2$  parallels (not equator) on the sphere, cutting it into 30 (alternatingly raised and depressed) pieces.

In the special case of the two families of sectorial harmonics, the undulations of the function become zero on the reference spheroid for  $\cos \varnothing = \pm 1$  (on the poles) and for  $\cos n\lambda = 0$ , i.e., along  $n$  meridians which are symmetrical to  $n$  planes through the rotational axis, thus cutting the spheroid in sectors which are alternately concave and convex.  $J_{4,4}$ , for example, would represent undulations featuring four meridians and eight sectors.

### C. The Harmonics Coefficients

The coefficients of the tesseral harmonics of the earth, especially the higher ones, are not really known. The sectorial coefficients  $J_{2,2}$  and  $J_{4,4}$  have been determined tentatively during the past 6 years and are sometimes used in high precision orbit determination programs<sup>5</sup>. For  $J_{2,2}$ , which has two zeros along a parallel (four sectors) and thus determines the ellipticity of the equator and the parallels, Kaula<sup>6</sup> gives

$$J_{2,2} = (1.80 \pm 0.1) \times 10^{-6}.$$

Of the tesseral harmonic perturbations of satellite orbits, only the sectorial  $J_{2,2}$  is large enough to be of practical concern in most orbit analyses; specifically, for example, this harmonic affects the supplemental energy requirements of 24-hour satellites. The sectorial harmonic due to  $J_{2,2}$  is depicted in figure 1.

Because of the uncertainty in and relative insignificance of the tesseral harmonics coefficients, they are usually neglected in the potential function which therefore assumes the commonly used form

$$U = \frac{\mu}{r} \left[ 1 - \sum_{n=1}^{\infty} J_n \cdot \left( \frac{\bar{R}_e}{r} \right)^n \cdot P_n(\sin \varnothing) \right] \quad (8)$$

which was first suggested by Brouwer<sup>7</sup> and adopted by the IAU in 1961. If so desired, tesseral and sectorial terms with the appropriate associated Legendre polynomials can be added to the second part of the equation, as required by the inclusion of the longitude  $\lambda$  in the analysis, as well as the rotational potential  $(1/2)r^2\omega^2\cos^2\varnothing$  to the whole equation to transform the gravitational potential in inertial coordinates for a free body to the gravity potential for a body attached to the earth.

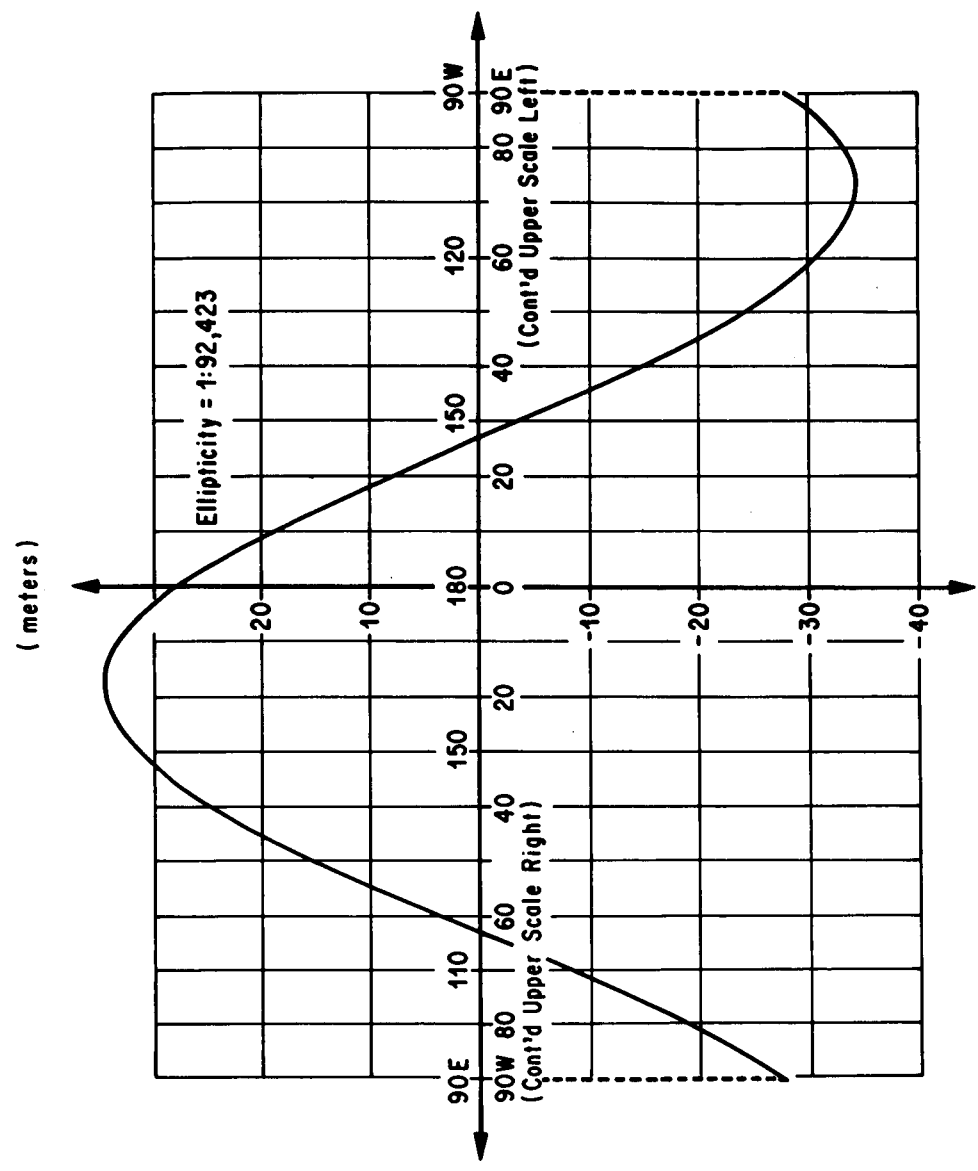


FIG. 1. FIRST SECTORIAL HARMONIC (DUE TO  $J_{2,2}$ ) AT EQUATOR

Of the (theoretically infinitely many) zonal harmonics coefficients  $J_n$ , only a few are known with adequate accuracy. If an equatorial geocentric coordinate system is assumed as a reference system such that its origin coincides with the center of mass, and if the latitude  $\varnothing$  is measured relative to this center, the first term in the sum of equation (8), which is proportional to  $1/r$ , vanishes since the coefficient  $J_1$ , multiplied with  $\bar{R}_e$ , would represent the distance between coordinate origin and center of mass; thus,  $J_1 = 0$ .

Of the other zonal functions, the second order harmonic is by far the largest, since it refers to the mass distribution due to the earth oblateness, thus defining the departure of the shape of an earth ellipsoid from that of an ideal sphere, while  $J_4$  being three orders of magnitude smaller than  $J_2$ , and all following even  $J$ 's account for deviations in hemispherical mass distribution symmetrical about the equator plane, i.e., for deviations of the geoid from the ellipsoid. Each even  $J$  of increasing order, while maintaining symmetry about the equator plane, "narrows down" the figure into an increasingly complex shape, while the sum of subsequent even  $J$ 's describe the deviation of the geoid from the preceding shape. The even  $J$ 's, however, all represent spheroid shapes with identical northern and southern "hemispheres."

The asymmetry of the northern and southern "hemispheres" of the geoid, also referred to as "pear" shape, is taken into account by the odd surface harmonics, which contain odd powers of  $\sin \varnothing$ , especially by the principal coefficient,  $J_3$ . Higher-odd-order  $J$ 's are at least one order of magnitude smaller than this coefficient.

The first zonal harmonic is shown in figure 2\*. Figures 3 and 4 depict the zonal harmonics due to  $J_3$  and  $J_4$ , and  $J_5$  and  $J_6$ , respectively. Of particular interest is the ovoid form of  $J_3$ , which is responsible for the "pear" shape of the earth.

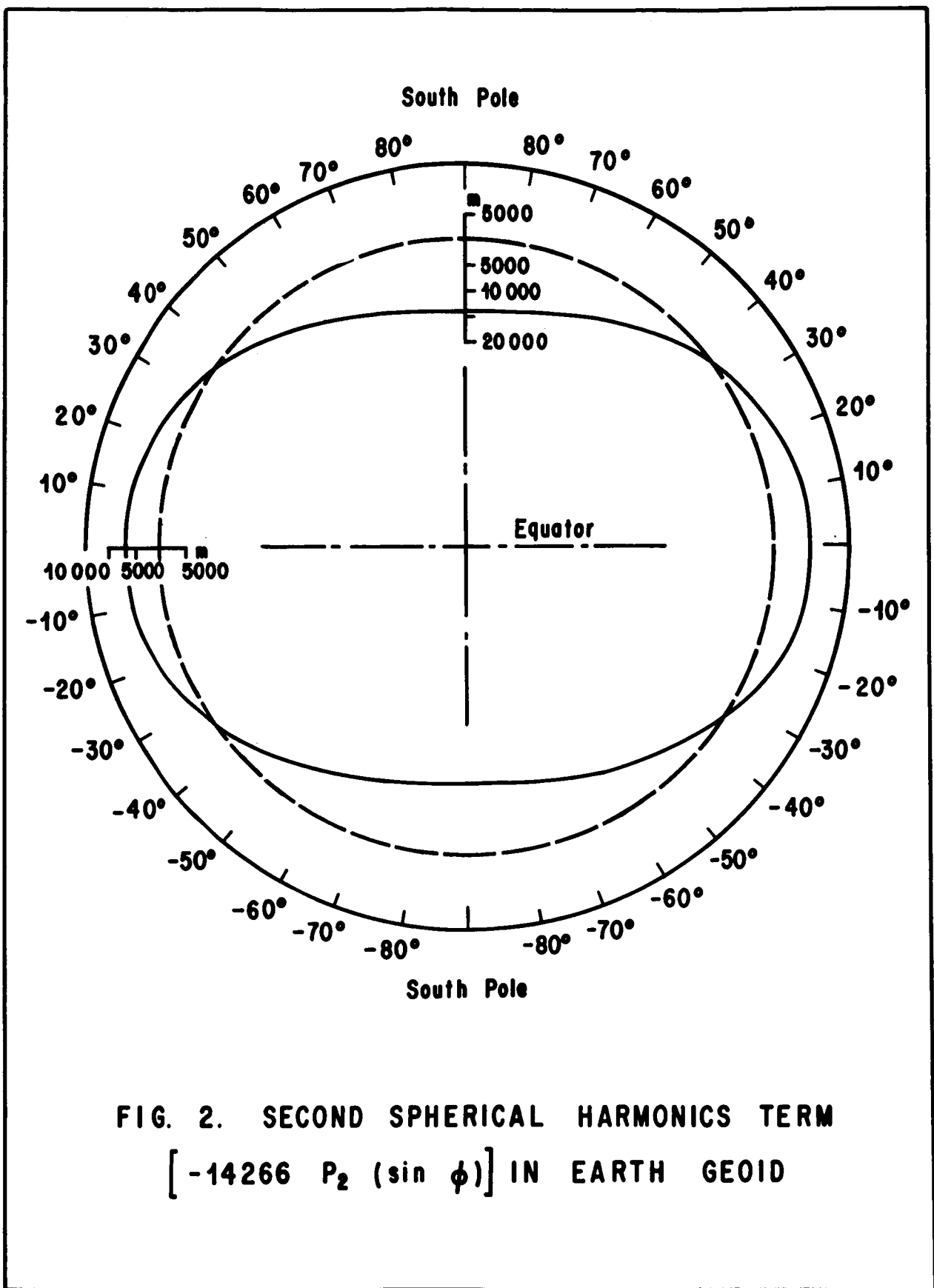
#### D. The Theorem of Clairaut

In the past, higher order zonal harmonics, and especially the odd harmonics, have been neglected in the geopotential. This was mainly due to the methods of determining the coefficients used before the advent of the artificial earth satellites. Also, since the amplitudes of high harmonics -- according to the quantity  $1/r^n$  in their terms -- decay very rapidly with altitude above the surface, and their effect on bodies in the earth's external gravitation field dwindles rapidly with increasing order and/or altitude, coefficients above fourth order, as well as the odd term  $J_3$ , were usually neglected. Before the advent of the artificial satellites, the moon was the only moving body in the earth's potential, but at its distance only the second harmonic is still discernible in its motion.

---

\* The figure is actually the second term of equation (34).





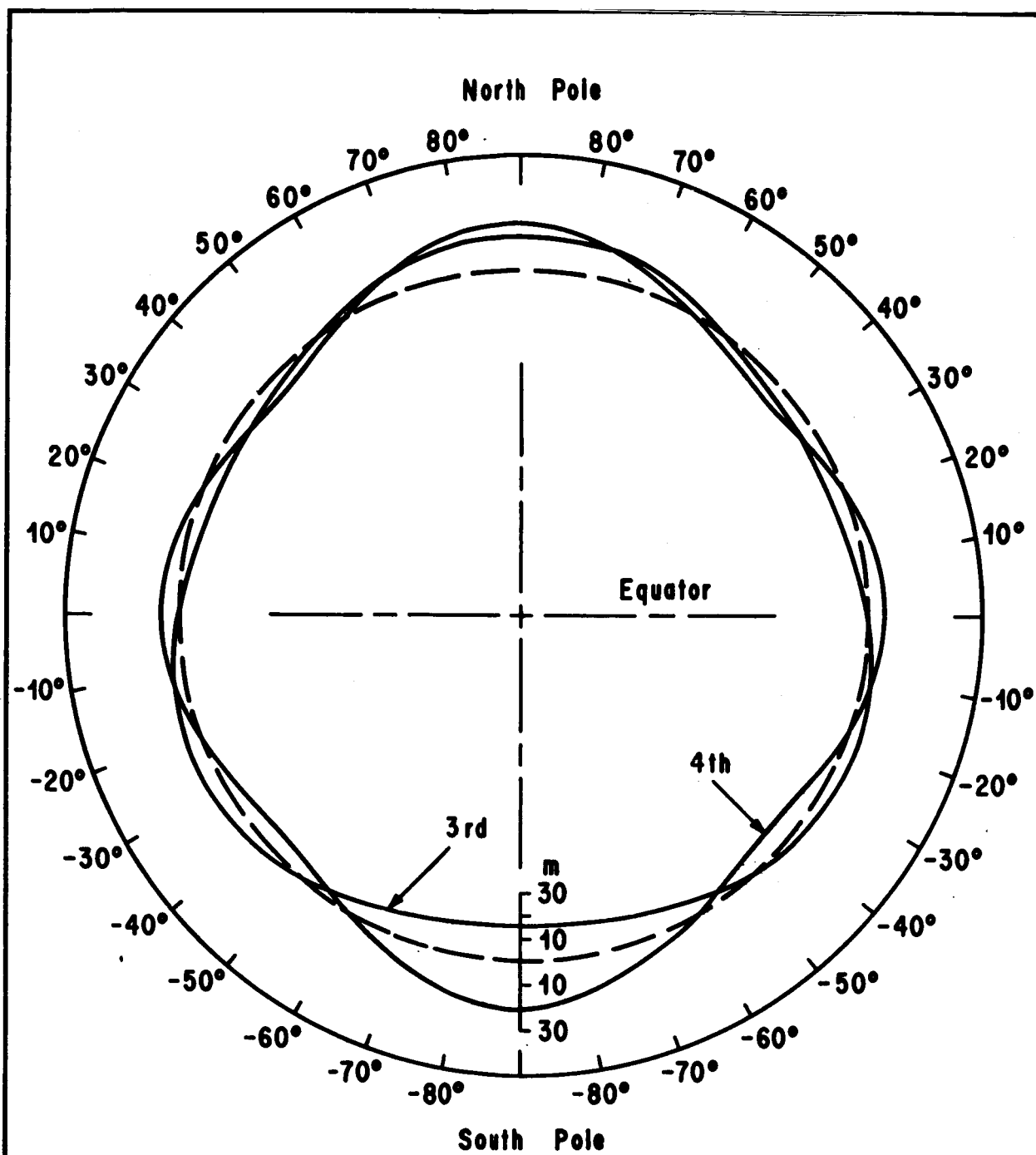


FIG. 3. THIRD AND FOURTH ORDER SPHERICAL HARMONICS TERMS  $[ 16 P_3 (\sin \phi); 20 P_4 (\sin \phi) ]$  IN EARTH GEOID

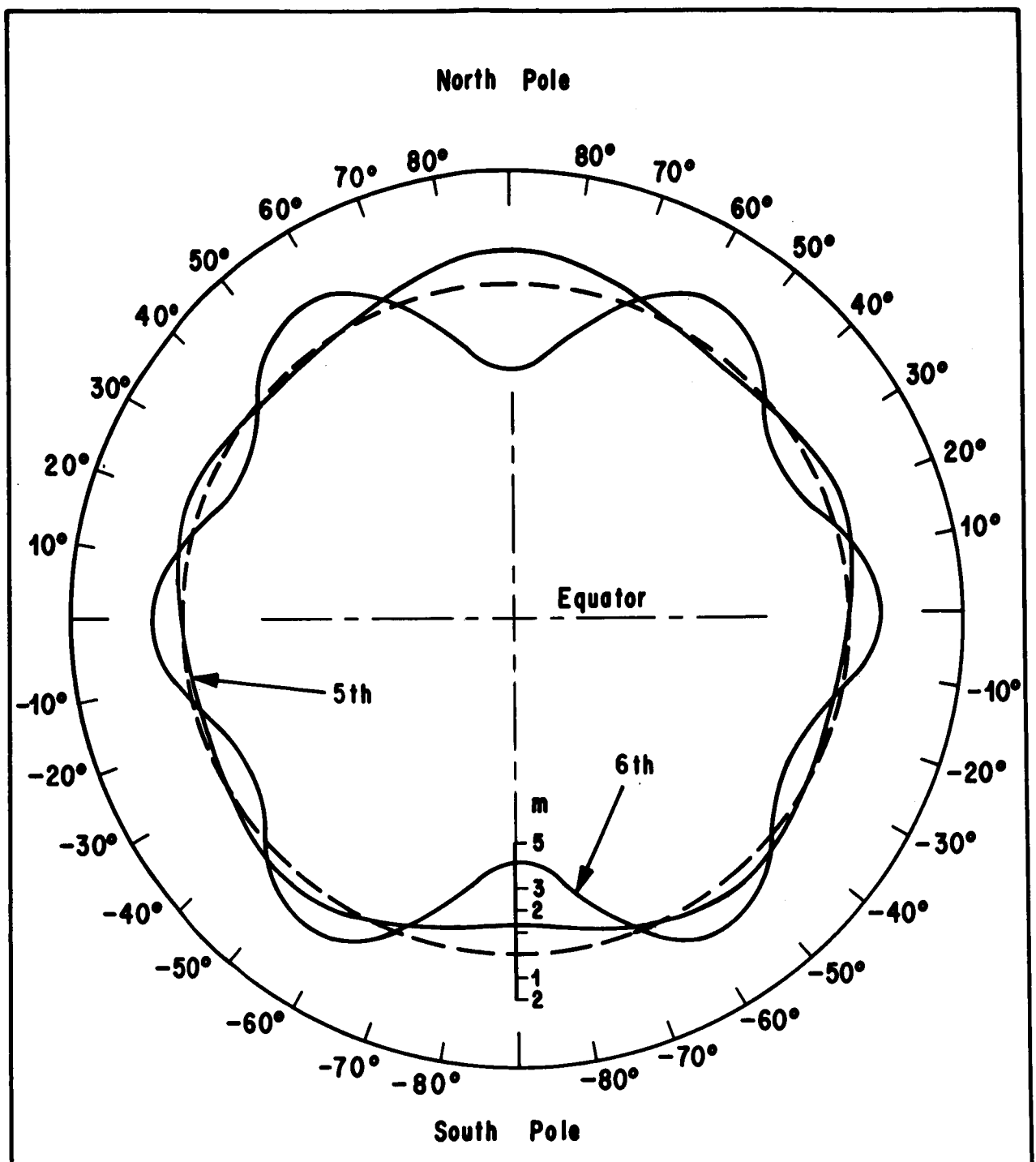


FIG. 4. FIFTH AND SIXTH ORDER SPHERICAL HARMONICS TERMS  $[1.3 P_5 (\sin \phi); -4 P_6 (\sin \phi)]$  IN EARTH GEOID

Determinations of the J-coefficients  $J_2$  and  $J_4$  were fundamentally based on geodetic surveys, gravity measurements, observations of the moon, and Clairaut's theorem. The latter deals with the form of a surface which encloses all the matter of a rotating body with various density distributions, which constitutes an equipotential surface (surface of constant potential). Clairaut's formula (1743) is

$$J = f - \frac{1}{2} m, \quad (9)$$

where  $J$  is the second harmonics coefficient,  $m$  is the centrifugal factor at the equator  $\omega^2 R / g_e$  (with  $\omega^2 R =$  centrifugal acceleration at equator,  $g_e =$  gravitational acceleration at equator), and  $f$  is the flattening of the ellipsoid of revolution, as assumed here.

Obviously, Clairaut's formula relates the amplitude of the second harmonic in gravity to that of the corresponding harmonic in the radius vector of the equipotential surface.

Clairaut's formula, because of the approximations made in deriving it, is not accurate enough for practical use. A second order extension of the theorem has been derived by Darwin (1899), DeSitter (1924), Jeffreys (1954), Bullen (1946), Cook (1959), et al., resulting in equations involving higher orders of the flattening, such as the third-order equation given by Kaula<sup>1</sup>,

$$J_2 = \frac{2}{3} f \left(1 - \frac{1}{2} f\right) - \frac{1}{3} m \left[1 - \frac{3}{2} m - \frac{2}{7} f + \frac{9}{4} m^2 + \frac{11}{49} f^2 + O(f^3)\right] \quad (10)$$

With the use of Clairaut's theorem, as well as its extensions by the mentioned authors, the earth flattening -- before the artificial satellites -- could be derived separately in two ways: from a harmonic analysis of observed gravity values (where the measured gravity anomalies are used to compute the absolute deflections of the vertical and, thus, the true undulations of the geopotential surface; also, to derive the detailed gravity field) and from astronomical observations of the constant of precession and the theory of the moon's motion (DeSitter, 1915), leading to  $J_2$ . Higher  $J$ 's could then be computed from the higher-order extensions of Clairaut's theorem, using the derived flattening, but when

the first artificial satellites were flown, it was found that higher-order harmonic coefficients determined with this method did not agree with the  $J$ 's actually observed from the orbital perturbations of the satellites. The reason for this serious discrepancy is simply the fact that for the higher-order terms, due to the irregular density distribution within the earth, the basic assumption of an ellipsoid of revolution as the figure of the earth in the Clairaut formula and all higher-order extensions is an increasingly bad approximation of the geoid.

#### E. The Geoid

Distinction is made between the geodetic geoid, which depends on the surface irregularities of the earth, and the geophysical geoid, which is governed by the internal irregular mass distribution of the earth.

The geodetic geoid is the true figure of the earth. While the actual earth surface with its irregularities is not an equipotential surface, the geophysical geoid, however, is required to be an equipotential level, identical with mean sea level and its continuation under the continents. The geoid, thus, is an extremely complex shape, requiring a very large number of higher-order harmonics for its description.

The reason for the use of the geoid in geodesy is the following: In principle, the geometrical form of the earth's surface can be found independent of observations of the potential and gravity, by geodetic triangulation methods, and then, given the values of these quantities on the surface, Laplace's equation can be solved for all the exterior space. Because of the extreme complexity of the true boundary, this would be an almost hopeless task. It is therefore universal practice to refer all geodetic observations to the gravitational equipotential surfaces and to determine the form of these from geodetic observations. Because the sea-level equipotential surface is an internal surface on land, the gravity field is not computed for the actual earth but for a model earth which is related to the actual earth and which is bounded by an equipotential surface. The field so computed will not agree with that of the actual earth throughout space, but the model may be chosen so that it agrees where observations can be made. This is the geoid.

The geodetic geoid must be computed point by point and cannot be given by few parameters, since it is not a mathematical surface but depends on the irregular distribution of visible and invisible masses near the earth's surface. For geodetic surveys, however, this point-by-point calculation would be impractical. Therefore, reference spheroids of revolution have been used instead. The reference spheroid is assumed to be an equipotential surface of the same volume and flattening as the geoid.

The history of geodesy has seen the following principal reference spheroids (all ellipsoids):

Germany (and several European states).....	1841.....	Bessel
England.....	1880.....	Clarke
U.S.S.R.....	1938.....	Krassowski
U.S.....	1866.....	Clarke
U.S.....	1910.....	Hayford
U.S.....	1963.....	Kaula/Fischer

#### F. Determination of the Harmonics Coefficients

As has been mentioned,  $J_2$  in former times was determined from the moon's motion. For the lower amplitudes of the higher order harmonics, however, these effects are not discernible because  $r$  becomes too large. However, when the first artificial satellites were orbited, it was found that the gravitational anomalies expressed by the higher-order harmonics characterize the potential field at their altitudes. Thus, the existence and magnitude of  $J_3$  (i.e., the "pear" shape of the earth) was first discovered from satellite 1958 $\beta$ 2 (Vanguard-1), launched in March 1958<sup>8</sup>.

The asphericity of the earth, represented by the spherical harmonics, causes constant secular and periodic perturbations on a satellite orbit. By observing the secular and periodic perturbations, the zonal harmonics coefficients can be determined. Since the secular changes, especially the orbital precession (i.e., the regressive rotation of the nodal line) and the advance of the perigee (i.e., the rotation of the apsidal line), depend primarily on the even-numbered  $J_n$ , while the long-period oscillations in four of the five orbital elements (eccentricity, inclination, longitude of ascending node (right ascension), and argument of perigee) are caused primarily by the odd harmonics<sup>9</sup>, the determination of the even  $J_n$  is usually done from secular changes, while the odd  $J_n$  are computed from periodic perturbations. An orbital perturbation suffered by one particular satellite yields one linear equation between the harmonics. For example, if  $\beta$  is the amplitude of the observed oscillation in eccentricity, we obtain an equation for the coefficients of the odd harmonics,  $J_3, J_5, J_7...$  of the form<sup>4</sup>

$$A_3J_3 + A_5J_5 + A_7J_7 + \dots = \beta, \quad (11)$$

where the A's are constants for a particular orbit and depend mainly on the orbital inclination  $i$  and semi-major axis  $a$ . By using several different satellites, several equations of the form (11) can be obtained. Therefore, if a large number of satellites (widely distributed over as many inclinations as possible) is available for analysis, an equally large number of  $J_n$  can be determined.

In solving the simultaneous equations (11), the main error of the analysis is introduced by the number of  $J_n$  to be determined remaining finite and all terms higher than the highest desired  $J$  being assumed negligible. In fact, however, these higher coefficients are not necessarily negligible, and since their effect is - by necessity - lumped together in the computed  $J_n$ , in any one analysis of a given set of satellites there are always several different solutions to the J's, depending on the number of J's considered in the algebraic equations. Thus, for example, King-Hele, et al.<sup>4</sup>, recently computed odd zonal harmonics up to  $J_{21}$  from eccentricity oscillations of 14 satellites, giving two different sets, i.e., one with  $J_3$  to  $J_{15}$ , and the other with  $J_3$  to  $J_{21}$ .

Also, the equations are sometimes solved by several different methods to obtain more confidence in the results. For example, the equations may be solved for three J's at a time, assuming the higher J's to be zero, in fours and fives, and also with least-squares and minimum-residual methods. The coefficients given by King-Hele<sup>4</sup> in the larger set are

$$\left. \begin{aligned}
 J_3 &= (-2.50 \pm 0.01) \times 10^{-6} \\
 J_5 &= (-0.26 \pm 0.01) \times 10^{-6} \\
 J_7 &= (-0.40 \pm 0.02) \times 10^{-6} \\
 J_9 &= ( 0 \pm 0.06) \times 10^{-6} \\
 J_{11} &= (-0.27 \pm 0.06) \times 10^{-6} \\
 J_{13} &= (+0.36 \pm 0.08) \times 10^{-6} \\
 J_{15} &= (-0.65 \pm 0.10) \times 10^{-6} \\
 J_{17} &= (+0.30 \pm 0.08) \times 10^{-6} \\
 J_{19} &= ( 0 \pm 0.11) \times 10^{-6} \\
 J_{21} &= (+0.58 \pm 0.11) \times 10^{-6}
 \end{aligned} \right\} \quad (12)$$

The latest most complete set of zonal harmonics, both even and odd coefficients, has been evaluated by Kozai. In 1963, Kozai<sup>10</sup> derived a set of values for eight coefficients of zonal harmonics (up to and

and including  $J_9$ ) from the (then) available observations of secular motions of the node and the perigee and the amplitudes of long-periodic terms of artificial satellites. Later, in 1964, from precisely reduced Baker-Nunn observations of nine high-inclination satellites ( $28^\circ - 95^\circ$ ), he produced<sup>11</sup> a new set of thirteen coefficients (up to  $J_{14}$ ):

$$\left. \begin{aligned}
 J_2 &= (1082.645 \pm 0.006) \times 10^{-6} & J_3 &= (-2.546 \pm 0.020) \times 10^{-6} \\
 J_4 &= (-1.649 \pm 0.016) \times 10^{-6} & J_5 &= (-0.210 \pm 0.025) \times 10^{-6} \\
 J_6 &= (+0.646 \pm 0.030) \times 10^{-6} & J_7 &= (-0.333 \pm 0.039) \times 10^{-6} \\
 J_8 &= (-0.270 \pm 0.050) \times 10^{-6} & J_9 &= (-0.053 \pm 0.060) \times 10^{-6} \\
 J_{10} &= (-0.054 \pm 0.050) \times 10^{-6} & J_{11} &= (+0.302 \pm 0.035) \times 10^{-6} \\
 J_{12} &= (-0.357 \pm 0.047) \times 10^{-6} & J_{13} &= (-0.114 \pm 0.084) \times 10^{-6} \\
 J_{14} &= (+0.179 \pm 0.063) \times 10^{-6} & &
 \end{aligned} \right\} \quad (13)$$

The values of Kozai's even coefficients have been compared recently<sup>12</sup> with two other sets of King-Hele/Cook and Smith. The agreement is excellent for all inclinations greater than  $28^\circ$ , which was the smallest inclination of available satellite orbits. It is therefore concluded that, as long as there are no satellites at inclinations between  $10^\circ$  and  $25^\circ$ , the evaluation of the even harmonics in the potential carried beyond the present status does not seem worthwhile. For the odd harmonics, this is not the case, since their primary effects, the long-periodic changes (e.g., the amplitude of the oscillation in eccentricity) decrease to zero as the inclination tends to zero. For this reason, King-Hele felt justified to publish the odd zonal harmonics to  $J_{21}$ , as given above, with an indication that  $J_{23}$  and  $J_{25}$  are small.

#### G. Krause's Theory of the Geoid Surface

If Kozai's value for  $J_2$ ,

$$J_2 = (1082.645 \pm 0.006) \times 10^{-6},$$

is introduced in a relation of a third-order Clairaut theory<sup>1</sup>,

$$J_2 = \frac{2}{3} f \left( 1 - \frac{1}{2} f \right) - \frac{1}{3} m \left[ 1 - \frac{3}{2} m - \frac{2}{7} f + \frac{9}{4} m^2 + \frac{11}{49} f^2 + 0(f^3) \right], \quad (14)$$



a value of  $f = 1/298.254$  results for the flattening of the reference earth ellipsoid. Using this  $f$  to compute the theoretical value of  $J_4$  for the reference ellipsoid assumed to be in hydrostatic equilibrium, one obtains  $-2.350 \times 10^{-6}$ , as compared to the observed value of  $-1.649 \times 10^{-6}$ . This discrepancy illustrates the increasing inaccuracy of Clairaut's (ellipsoid) theorem and its extension, if applied to higher-order harmonics.

To find a more accurate relation between the radius vector of the earth and its gravity field, thereby cleaning up the inconsistency in the older theories, Krause recently developed a new theory<sup>13,14</sup> which essentially introduces the radius vector of the geoid, rather than of an ellipsoid, consistently expressed to the same accuracy as the potential field it is related to. Since the new theory is kept general, it can handle all higher order zonal harmonics up to  $J_n$  with the same internal consistency, which the older theories, based on Clairaut, Darwin, Helmert, et al., are unable to do. Using Krause's theory with Kozai's thirteen coefficients and introducing the radius vector of the geoid expanded in spherical harmonics up to  $J_{14}$  in the similarly expanded geopotential, a new flattening of the earth can be computed,  $f = 1/298.1840^*$ , which differs both from the old second-order value given above and from the flattening of the Kaula/Fischer ellipsoid used currently as a world datum, for example, in trajectory computations ( $1/298.30$ ). It is believed that the value derived with Krause's theory is more consistent with the observed spherical harmonics coefficients.

In his theory<sup>13,14</sup>, Krause has made use of the fact that the generalized (equipotential) surface of the geoid, similarly to the geopotential, can be represented alternatively by two series expansions, one consisting of spherical harmonics, the other of powers of the sine of the latitude. When introduced in the geopotential, the chosen series must be of the same degree as the potential function used. The author shows that the coefficients of the terms of the series ( $A_n$  in the spherical harmonics series,  $B_n$  in the power series) are related to the known oblateness coefficients  $J_n$  of the geopotential equation  $U$  and can be computed from these. Insertion of the radius equation thus obtained in the equation of the total gravity acceleration in the direction of the normal yields the gravitational acceleration of the geoid as an expansion of surface harmonics, based on a consistent geoid geometry. Because of the relation between the  $A_n$  (or  $B_n$ ) coefficients and the oblateness coefficients  $J_n$ , and assuming the surface to be of constant potential, the oblateness of the northern and southern "hemispheres" and,

---

\*The value given in references 13 and 14 has been slightly corrected by the present writer.

thus, the mean meridional flattening  $f$  can be computed from the  $A_n$  coefficients, relating now to the true geoid and the full set of observed  $J_n$ , rather than to a reference ellipsoid, as in Clairaut's theory.

For the geoid radius, expanded in spherical harmonics,

$$\frac{R}{\bar{R}_e} = A_0 - \sum_{n=1}^{\infty} A_n P_n(\sin \varphi) + 3A_{2,2} \cos^2 \varphi \cos 2(\lambda - \lambda_0), \quad (15)$$

in which the first sectorial harmonic, with the associated Legendre polynomial  $P_2^2(\sin \varphi)$  exactly given by  $3 \cos^2 \varphi$ , is taken into account to express the ellipticity of the earth equator, Krause finds for the A-coefficients<sup>13,14</sup>:

$$A_0 = 1 - \frac{1}{\chi} \left[ - \sum_{\nu=1}^{\infty} (-1)^\nu \frac{1 \cdot 3 \cdot 5 \dots (2\nu - 1)}{2 \cdot 4 \cdot 6 \dots 2\nu} J_{2\nu} + \frac{1}{6} \tilde{\omega}_e + \frac{1}{5} B_2 \left( \frac{9}{2} J_2 - \tilde{\omega}_e - B_2 \right) \right] \quad (16)$$

$$A_2 = \frac{1}{\chi} \left[ J_2 + \frac{1}{3} \tilde{\omega}_e + \frac{4}{7} B_2 \left( \frac{9}{2} J_2 - \tilde{\omega}_e - B_2 \right) \right] \quad (17)$$

$$A_4 = \frac{1}{\chi} \left[ J_4 + \frac{8}{35} B_2 \left( \frac{9}{2} J_2 - \tilde{\omega}_e - B_2 \right) \right] \quad (18)$$

$$A_k = \frac{1}{\chi} J_k \quad (k \neq 0, 2, 4) \quad (19)$$

where

$$\tilde{\omega}_e = \frac{\omega^2 \cdot \bar{R}_e^3}{GM} = \text{centrifugal factor at equator}, \quad (20)$$

$$B_2 = \frac{1}{\chi} \left[ \sum_{\nu=0}^{\infty} (-1)^\nu \frac{1 \cdot 3 \cdot 5 \dots (2\nu + 3)}{2^\nu \nu! 2!} J_{2\nu+2} + \frac{1}{2} \tilde{\omega}_e \right], \quad (21)$$

and

$$\chi = 1 - \sum_{n=1}^{\infty} (-1)^n \frac{3 \cdot 5 \cdot 7 \dots (2n+1)}{2 \cdot 4 \cdot 6 \dots 2n} J_{2n} - \tilde{\omega}_e. \quad (22)$$

If the first variation of  $U$  with longitude, as represented especially by the first sectorial term, is taken into account as it was in equation (15), where  $3 \cos^2 \varphi$  is used as an exact substitute of  $P_2^2(\sin \vartheta)$ , the geopotential of the earth becomes in inertial coordinates

$$U = \frac{GM}{r} \left[ 1 - \sum_{n=2}^{\infty} J_n \left( \frac{\bar{R}_e}{r} \right)^n P_n(\sin \vartheta) + 3J_{2,2} \left( \frac{\bar{R}_e}{r} \right)^2 \cos^2 \varphi \cos 2(\lambda - \lambda_0) + \frac{1}{2} \tilde{\omega}_e \cos^2 \varphi \right]. \quad (23)$$

Since the three components (in polar coordinates) of the gravity are defined as

$$\begin{aligned} g_r &= \frac{\partial U}{\partial r} \\ g_\lambda &= \frac{1}{r \cos \varphi} \frac{\partial U}{\partial \lambda}, \\ g_\varphi &= \frac{1}{r} \frac{\partial U}{\partial \varphi} \end{aligned} \quad (24)$$

while the total gravity acceleration in the direction of the normal is

$$g = \sqrt{g_r^2 + g_\lambda^2 + g_\varphi^2}, \quad (25)$$

the gravity, including the sectorial term, can be given by determining the potential derivatives and expanding the sum of their squares according to equation (25) in a series approximating the square-root of equation (25). The result is<sup>13,14</sup>

$$\begin{aligned}
 g = \frac{GM}{r^2} & \left\{ 1 - \sum_{n=2}^{\infty} (n+1) J_n \left( \frac{\bar{R}_e}{r} \right)^n \cdot P_n(\sin \vartheta) \right. \\
 & + 9 J_{2,2} \left( \frac{\bar{R}_e}{r} \right)^2 \cos^2 \vartheta \cos 2(\lambda - \lambda_0) - \tilde{\omega}_e \left( \frac{r}{\bar{R}_e} \right)^3 \cos^2 \vartheta \\
 & \left. + \frac{1}{2} \left[ 3J_2 \left( \frac{\bar{R}_e}{r} \right)^2 + \tilde{\omega}_e \left( \frac{r}{\bar{R}_e} \right)^3 \right]^2 \sin^2 \vartheta \cos^2 \vartheta \right\}, \quad (26)
 \end{aligned}$$

where only the derivative of  $P_2(\sin \vartheta)$  with respect to  $\vartheta$  has been included (expressed as

$$P_2'(\sin \vartheta) = \frac{dP_2(\sin \vartheta)}{d\vartheta} = 3 \sin \vartheta \cos \vartheta,$$

while the higher order derivatives have been neglected.

### III. ANALYSIS OF MODELS

#### A. Model 1 (J<sub>2</sub>-Only)

For computation of trajectories close to earth, featuring small central range angles, the effects of the equatorial bulge and other irregularities can usually be considered negligible, primarily because the flight times involved are relatively short. In this model, it is therefore assumed that the earth is an ellipsoid of revolution, symmetrical around all three axes. Except for the second harmonic, all higher order effects of asphericity (which are three or four orders of magnitude smaller than J<sub>2</sub>) are taken as zero.

With these assumptions, the gravity equation (26) reduces to

$$g = \frac{GM}{r^2} \left\{ 1 - 3J_2 \left( \frac{R_e}{r} \right)^2 P_2(\sin \vartheta) - \tilde{\omega}_e \left( \frac{r}{R_e} \right)^3 \cos^2 \vartheta \right. \\ \left. + \frac{1}{2} \left[ 3J_2 \left( \frac{R_e}{r} \right)^2 + \tilde{\omega}_e \left( \frac{r}{R_e} \right)^3 \right]^2 \sin^2 \vartheta \cos^2 \vartheta \right\}. \quad (27)$$

It would be more accurate to compute the gravity directly from the potential of the ellipsoid, rather than from the series approximation, equation (27). The task of determining the potential of a homogeneous ellipsoid was a very formidable one and remained unsolved till the end of the 18th century, despite attempts at a solution by Newton, Maclaurin, D'Alembert and Lagrange. Finally, Laplace succeeded in finding the general solution, followed later by Gauss and others. The general form of the potential of a homogeneous, triaxial ellipsoid for an exterior point involves an elliptic integral of the first kind; hence, the components of the gravity force of the ellipsoid also contain elliptic integrals. For the present case of the ellipsoid of revolution, the equations become considerably simpler; the elliptic integrals reduce to logarithmic-cyclometric integrals. The investigations of the above mentioned authors generally refer to homogeneous bodies. Clairaut was the first who investigated inhomogeneous bodies.

A third-order relation of Clairaut's theory is given by Kaula<sup>1</sup>:

$$J_2 = \frac{2}{3} f \left( 1 - \frac{1}{2} f \right) - \frac{1}{3} m \left[ 1 - \frac{3}{2} m - \frac{2}{7} f + \frac{9}{4} m^2 + \frac{11}{49} f^2 + 0(f^3) \right]. \quad (28)$$

Kaula gives also

$$\left. \begin{aligned} GM_{\oplus} &= 3.986032 \times 10^{20} \text{ cm}^3 \text{ sec}^{-2} \\ &= 398603.2 \text{ km}^3 \text{ sec}^{-2} \\ \omega &= 0.729,211,585 \times 10^{-4} \text{ sec}^{-1} \\ R_e &= 6378165.0 \text{ m} \\ g_e &= 978.0300 \text{ cm} \cdot \text{sec}^{-2} \end{aligned} \right\}. \quad (29)$$

Using these values, the centrifugal factor at the equator,  $m$ , becomes

$$m = \frac{\omega^2 \cdot R_e}{g_e} = 0.003,467,773,255, \quad (30)$$

which is in agreement with reference 6.

For Model 1, the value for  $J_2$  used is the first one of the set given recently by Kozai<sup>11</sup>, equation (13):

$$J_2 = 1082.645 \times 10^{-6}. \quad (31)$$

In a strict sense, this  $J_2$ -value is not completely consistent with the above given value of  $g_e$  from Kaula<sup>1</sup>. The equatorial gravity of the oblate spheroid may be computed from

$$g_e = \sigma \cdot \frac{GM_{\oplus}}{R_e},$$

where the factor  $\sigma$  accounts for two effects. First, it includes a correction to  $M_{\oplus}$  because the mass of the earth's atmosphere, included in  $M_{\oplus}$ , does not contribute to the gravitational acceleration at the surface, and second, it modifies the succeeding term, valid for a sphere only, for the oblateness effects. In the Kaula value of equation (29),  $\sigma$  by necessity refers to the older  $J_2$  and probably also to the older  $J_4$ . However, the inconsistency is not felt to be of practical consequence for the present purpose. For the  $J_2$  of equation (31),  $\sigma$  would become 0.9981616959 (by solving equation (22) and computing  $\sigma = \chi(1 - A)$ , where  $A = M_{\text{atm}}/M_{\oplus} = 0.8594 \times 10^{-16}$ )<sup>14</sup>, so that the above equation results in  $g_e = 978.026$  gal, 4 mgal lower than Kaula's value, which is presently accepted as standard<sup>15</sup>.

It must be kept in mind that the assumption of all higher  $J_n$  being zero introduces, in the strict sense, an error in the model which is not taken into account by the above  $J_2$ -coefficient, since its particular value has been determined from simultaneous algebraic equations involving 12 additional coefficients of higher order, which were different from zero. However, it is assumed that the uncertainty caused by this fact will be of no concern for the present purposes. This assumption is justified by the results of this analysis.

Introducing the  $J_2$ -value in equation (28), one obtains the oblateness

$$f = 0.0033528465 = 1 : 298.254,$$

which is consistent with the assumed geopotential.

With the value for  $R_e$  given in equation (29), the polar earth radius becomes

$$R_p = R_e (1 - f) \quad (32)$$

$$R_p = 6356780.0 \text{ m}$$

$$R_e = 6378165.0 \text{ m}$$

and the general radius at latitude  $\varnothing$

$$R = \frac{R_e R_p}{\sqrt{R_p \cos^2 \varnothing + R_e \sin^2 \varnothing}} \quad (33)$$

Since the assumption of an ellipsoid is not fully consistent with the gravitation assumed (based on  $J_2$ ), a second body has been determined by using the first spherical harmonic in a truncated expression of the type (15). By solving equations (16), (17), (20), (21) and (22), the coefficients are determined:

$$A_0 = 0.9988810301$$

$$A_1 = 0$$

$$A_2 = 0.2236813952 \times 10^{-2}$$

$$A_3 = 0$$

$$A_4 = -0.1501014034 \times 10^{-5}.$$

Neglecting the coefficient  $A_4$ , the radius of the spheroid is then determined from

$$R_1 = 6371028.026 - 14266.76846 \cdot P_2(\sin \varnothing), \quad (34)$$

where  $P_2(\sin \varnothing)$  is the second-degree Legendre polynomial.

The resulting spheroid is depicted in figure 5.

The total gravity (equation (27)) and the surface shape of the ellipsoidal Model 1 (equation (33)), as well as the surface of the body formed by the  $J_2$ -harmonic (equation (34)) are given in table 1.

#### B. Model 2 (NASA Standard)

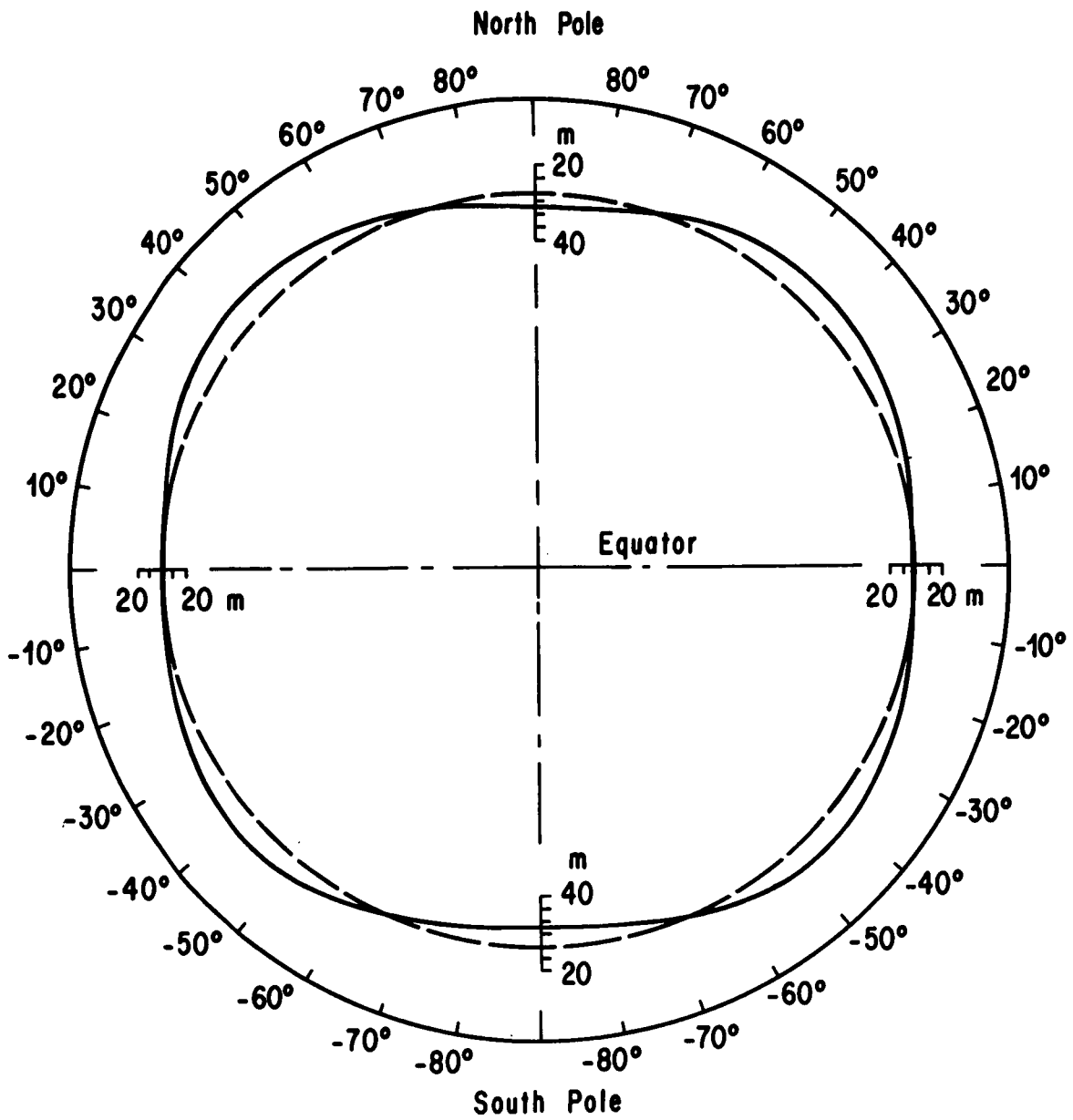
For trajectories of longer duration, such as those of upper stages, as well as for near-earth orbits, the geopotential exhibits anomalies such that its effect deviates from that of an attracting ellipsoid of revolution. For almost all practical purposes, however, it suffices to add only the two next higher-order zonal harmonics to the potential and to consider the gravity anomalies averaged over all longitudes, thus retaining the rotational symmetry around the polar axis and rendering tesseral and sectorial terms unnecessary.

The second model is represented by the geopotential and the astrogeodetic world datum as adopted by the Ad Hoc NASA Standard Constants Committee<sup>15</sup> in 1963 for Project Apollo and other NASA programs. The standard is based on the Kaula/Fischer Ellipsoid of 1963. Irene Fischer of the U. S. Army Map Service, in 1960, published a world ellipsoid based on an imposed flattening  $f = 1/298.30$  (which at that time appeared to be the best available value from early artificial satellites), by determining the ellipsoid of revolution which best fit the geoid contours derived from astrogeodetic measurements<sup>16</sup>. Kaula later<sup>1</sup>, in 1963, published a new value for the equatorial radius,

$$R_e = 6378165.0 \pm 25.0 \text{ m}, \quad (35)$$

which was a compromise between Fischer's value<sup>16</sup> and a 1961 value by Kaula<sup>17</sup>. The NASA Committee meeting at Goddard Space Flight Center in May 1963 adopted this value, along with the following constants<sup>15</sup>:





— =  $J_2$  - Spheroid  
 --- = Ellipsoid

FIG. 5. HEIGHT OF  $J_2$ -SPHEROID (MODEL 1) OVER REFERENCE ELLIPSOID OF FLATTENING 1/298.222 (MODEL 3)

TABLE 1

Model 1

Latitude North or South (deg)	Radius (Ellipsoid) (m)	Radius (Spheroid) (m)	Height of Sphe- roid over Ellipsoid (m)	Gravity (gal)
90 (poles)	6356780.0	6356761.3	-18.7	983.2049
85	6356941.6	6356923.8	-17.8	983.1663
80	6357421.7	6357406.6	-15.1	983.0516
75	6358205.8	6358194.8	-11.0	982.8641
70	6359270.5	6359264.6	- 5.9	982.6093
65	6360583.7	6360583.5	- 0.2	982.2944
60	6362106.1	6362111.3	5.2	981.9286
55	6363791.7	6363801.7	10.0	981.5228
50	6365589.7	6365603.3	13.6	981.0890
45	6367445.6	6367461.3	15.7	980.6401
40	6369303.1	6369319.4	16.3	980.1897
35	6371105.7	6371121.0	15.3	979.7517
30	6372798.5	6372811.4	12.9	979.3394
25	6374329.7	6374339.2	9.5	978.9656
20	6375652.3	6375658.1	5.8	978.6422
15	6376725.7	6376727.9	2.2	978.3794
10	6377517.0	6377516.1	- 0.9	978.1854
5	6378001.7	6377998.9	- 2.8	978.0664
0 (equator)	6378165.0	6378161.4	- 3.6	978.0300

$$\left. \begin{aligned}
 GM_{\oplus} &= 398603.2 \text{ km sec}^{-2} \\
 f &= 1 : 298.30 \\
 g_e &= 978.030 \text{ gal} \\
 J &= 1.62345 (\pm 0.00030) \times 10^{-3} \\
 H &= -0.575 (\pm 0.025) \times 10^{-5} \\
 D &= 0.7875 (\pm 0.0875) \times 10^{-5} \\
 R_p &= 6356783.3 \text{ m} \\
 \tilde{\omega}_e &= 3461.414_3 \times 10^{-6} \text{ sec}^{-1}
 \end{aligned} \right\} , \quad (36)$$

where the J, H, D coefficients apply to an alternate (older) form of the geopotential, and the value

$$\tilde{\omega}_e = \frac{\omega^2 R_e^3}{GM}$$

is fully consistent with the assumed parameters.

In the modern notation, the oblateness coefficients become

$$\left. \begin{aligned}
 J_2 &= \frac{2}{3} J = 1082.30 \times 10^{-6} \\
 J_3 &= \frac{2}{5} H = -2.30 \times 10^{-6} \\
 J_4 &= -\frac{8}{35} D = -1.80 \times 10^{-6}
 \end{aligned} \right\} . \quad (37)$$

It is pointed out that the above set of constants is consistent within itself for most practical purposes. However, since the geometrical figure assumed is still an ellipsoid of revolution (equal northern and southern "hemispheres"), derived from  $J_2$  through a third-order relation of Clairaut's theory (equation (28))<sup>1</sup>, it is at best only an approximation and contains theoretically an inconsistency.

Table 2 lists the gravity of Model 2 (second column), computed from equation (26) without the longitude-dependent term, with  $J_2$ ,  $J_3$ ,  $J_4$  as given by equation (37), and in the third column the local radius of the associated Kaula/Fischer reference ellipsoid, computed from equation (33) with the data given in (35) and (36).

As an illustration of the inherent inconsistency of the NASA Standard model, it is seen that the gravity field at the North Pole is higher by 18.4 mgal than at the South Pole, while the radial distance computed from the model is unable to account for this "pear" shape.

To compare the deviation of the ellipsoid from the (here assumed) geoid, the shape of the geoid must be computed. The new theory by Krause<sup>13,14</sup>, discussed in Section II, provides a relatively simple method for doing this. To write the geoid radius in an expansion of the second, third and fourth surface harmonics, the coefficients  $A_n$  in equation (15) must be determined with  $J_2$ ,  $J_3$ ,  $J_4$  (equation (37)), from equations (16) through (22).

One obtains

$$\left. \begin{aligned} A_0 &= 0.9988805375 \\ A_1 &= 0 \\ A_2 &= 0.2236440156 \times 10^{-2} \\ A_3 &= -0.2304227311 \times 10^{-5} \\ A_4 &= -0.3313107217 \times 10^{-5} \end{aligned} \right\} , \quad (38)$$

with which the geoid surface of Model 2 can be expressed by

$$\begin{aligned} R_g &= 6371024.88 - 14264.38 \cdot P_2(\sin \vartheta) + 14.69 \cdot P_3(\sin \vartheta) \\ &+ 21.13 \cdot P_4(\sin \vartheta) \quad (\text{m}) \end{aligned} \quad (39)$$

where the  $P_n(\sin \vartheta)$  are the Legendre polynomials of argument  $\sin \vartheta$ .

Column 4 of table 2 lists the results of equation (39), while the deviations of the ellipsoid from the geoid are given in column 5. It is seen that the NASA Standard Model results in an earth radius which is 13 m below the geoid at the North Pole, 16.4 m above the geoid at the South Pole, and between zero and 12 m above or below it in the intermediate latitudes.

TABLE 2  
Model 2

Latitude (degrees)	Gravity (gal)	Radius: Ellipsoid (m)	Radius Geoid (m)	Difference (m)
90N (pole)	983.2231	6356783.3	6356796.3	-13.0
85	983.1839	6356944.9	6356957.7	-12.8
80	983.0676	6357424.9	6357437.1	-12.2
75	982.8776	6358208.9	6358220.1	-11.2
70	982.6195	6359273.4	6359283.2	- 9.8
65	982.3011	6360586.4	6360594.6	- 8.2
N 60	981.9317	6362108.6	6362114.9	- 6.3
O 55	981.5225	6363793.9	6363798.3	- 4.4
R 50	981.0857	6365591.6	6365593.9	- 2.3
T 45	980.6346	6367447.2	6367447.6	- 0.4
H 40	980.1829	6369304.5	6369303.1	1.4
35	979.7444	6371106.8	6371104.0	2.8
30	979.3325	6372799.4	6372795.4	4.0
25	978.9598	6374330.3	6374325.7	4.6
20	978.6380	6375652.7	6375648.0	4.7
15	978.3770	6376726.0	6376721.7	4.3
10	978.1850	6377517.1	6377513.9	3.2
5	978.0678	6378001.8	6378000.0	1.8
0 (equator)	978.0300	6378165.0	6378165.0	0
5	978.0701	6378001.8	6378003.8	- 2.0
10	978.1895	6377517.1	6377521.1	- 4.0
15	978.3833	6376726.0	6376731.9	- 5.9
20	978.6455	6375652.7	6375660.1	- 7.4
25	978.9679	6374330.3	6374338.8	- 8.5
S 30	979.3404	6372799.4	6372808.3	- 8.9
O 35	979.7514	6371106.8	6371115.4	- 8.6
U 40	980.1884	6369304.5	6369311.9	- 7.4
T 45	980.6379	6367447.2	6367452.8	- 5.6
H 50	981.0862	6365591.6	6365594.7	- 3.1
55	981.5198	6363793.9	6363794.0	- 0.1
60	981.9257	6362108.6	6362105.4	3.2
65	982.2919	6360586.4	6360579.9	6.5
70	982.6074	6359273.4	6359263.7	9.7
75	982.8629	6358208.9	6358196.4	12.5
80	983.0509	6357424.9	6357410.3	14.6
85	983.1660	6356944.9	6356929.0	15.9
90S (pole)	983.2047	6356783.3	6356766.9	16.4

With

$$f = 1 - \left\{ \frac{R_{pN} + R_{pS}}{2\bar{R}_e} \right\}, \quad (40)$$

the mean meridional oblateness becomes

$$f = 0.0033525944 = 1 : 298.276, \quad (41)$$

differing slightly from the Standard value of 1 : 298.30.

The NASA Standard, here called Model 2, adopted by the Ad Hoc Committee in 1963, has served and is serving its purpose well, which is to ensure accuracy and consistency between the various NASA agencies and contractors participating in the space program. While during 1961-63 a real attempt was made to select a set of constants which might be termed the "best available at the time"<sup>15</sup>, the chief qualification of the adopted set was standardization. Since the adoption of the NASA Standard for Apollo and other space programs, new and better determinations of the geographical (and astrodynamic) constants have been made. The Standard of 1963, still valid today, is therefore not based on more current information; however, with the present status of the Apollo program, it would probably be ill-advised to update the Standard at this time.

The following models make use of the more recent determinations in various combinations.

### C. Model 3 (New $J_2, J_3, J_4$ )

Similar to the preceding analysis, a model is assumed which takes the "pear" shape of the earth into account as well as the second even zonal harmonic, but not any dependence of the geopotential on longitude. The spherical harmonics coefficients are taken from Kozai<sup>11</sup> (equation (13)),

$$\left. \begin{aligned} J_2 &= 1082.645 \times 10^{-6} \\ J_3 &= -2.546 \times 10^{-6} \\ J_4 &= -1.649 \times 10^{-6} \end{aligned} \right\}, \quad (42)$$

where they have actually been determined together with ten additional coefficients, which are here assumed zero. This introduces a slight error of no practical concern for the present purpose.

Gravity is again computed from equation (26), without the sectorial term, with  $J_2$ ,  $J_3$ ,  $J_4$  as given in (42).

According to the new J-coefficients, the  $\sigma$ -factor in the equation for the equatorial gravity acceleration must now be slightly adjusted;  $g_e$  becomes now

$$g_e = 978.029 \text{ gal}$$

instead of the Standard value 978.030 gal.

The reference ellipsoid (of revolution) postulated for this model is required to be consistent with the geopotential used.

Using Krause's theory, the A-coefficients (equations (16) through (22)) in equation (15) are obtained.

$$\left. \begin{aligned} A_0 &= 0.9988804206 \\ A_1 &= 0 \\ A_2 &= 0.2236788408 \times 10^{-2} \\ A_3 &= -0.2550678850 \times 10^{-5} \\ A_4 &= -0.3160571410 \times 10^{-5} \end{aligned} \right\}, \quad (43)$$

and the radius of the assumed geoid becomes

$$R_3 = 6371024.14 - 14266.61 P_2(\sin \varnothing) + 16.268 P_3(\sin \varnothing) + 20.16 P_4(\sin \varnothing) \quad (m). \quad (44)$$

The results of this equation for the geoid surface are listed in column 4 of table 3. It can be seen that the polar radii are

$$\begin{aligned} R_{pN} &= 6356794.0 \text{ m} \\ R_{pS} &= 6356761.4 \text{ m} \end{aligned}$$

TABLE 3

Model 3

Latitude (deg)	Gravity (gal)	Radius Ellipsoid (m)	Radius Geoid (m)	Difference (Height of Ellipsoid) (m)
90	983.2239	6356777.7	6356794.0	-16.3
85	983.1848	6356939.4	6356955.4	-16.0
80	983.0685	6357419.5	6357434.8	-15.3
75	982.8786	6358203.7	6358217.9	-14.2
70	982.6205	6359268.4	6359281.2	-12.8
65	982.3020	6360581.8	6360592.8	-11.0
N 60	981.9326	6362104.3	6362113.3	- 9.0
55	981.5234	6363790.1	6363796.8	- 6.7
O 50	981.0866	6365588.3	6365592.6	- 4.3
R 45	980.6354	6367444.4	6367446.4	- 2.0
T 40	980.1835	6369302.1	6369302.0	0.1
35	979.7449	6371105.0	6371103.0	2.0
H 30	979.3328	6372797.9	6372794.5	3.4
25	978.9601	6374329.3	6374324.9	4.4
20	978.6382	6375652.0	6375647.3	4.7
15	978.3771	6376725.6	6376721.2	4.4
10	978.1851	6377516.9	6377513.5	3.4
5	978.0679	6378001.7	6377999.8	1.9
0	978.0294	6378165.0	6378165.0	0
5	978.0705	6378001.7	6378004.0	- 2.3
10	978.1900	6377516.9	6377521.5	- 4.6
15	978.3840	6376725.6	6376732.4	- 6.8
20	978.6464	6375652.0	6375660.8	- 8.8
25	978.9689	6374329.3	6374339.4	-10.1
S 30	979.3416	6372797.9	6372808.8	-10.9
35	979.7527	6371105.0	6371115.6	-10.6
O 40	980.1896	6369302.1	6369311.8	- 9.7
U 45	980.6389	6367444.4	6367452.2	- 7.8
T 50	981.0871	6365588.3	6365593.4	- 5.1
55	981.5205	6363790.1	6363792.1	- 2.0
H 60	981.9261	6362104.3	6362102.7	1.6
65	982.2919	6360581.8	6360576.5	5.3
70	982.6070	6359268.4	6359259.6	8.8
75	982.8623	6358203.7	6358191.8	11.9
80	983.0501	6357419.5	6357405.2	14.3
85	983.1650	6356939.4	6356923.6	15.8
90	983.2037	6356777.7	6356761.4	16.3



so that the mean meridional flattening, equation (40), becomes

$$f = 0.003353206 = 1 : 298,222.$$

Comparison with the geoid of Model 2 shows that the new values for  $J_2$ ,  $J_3$ ,  $J_4$  cause the Model 3 geoid to be smaller at most latitudes (by 2.3 m at the North Pole, 5.5 m at the South Pole, and by 1.2 m and 0.6 m at 45N and 45S, respectively).

For the reference ellipsoid, the equator radius imposed is the currently accepted value due to Kaula, equation (35). With the above flattening, the polar radius of the ellipsoid then becomes

$$R_p = R_e (1 - f) = 6356777.70 \text{ m},$$

and the ellipsoid shape can then be computed from equation (33). Results are listed in column 3 of table 3. The deviations of the ellipsoid from the geoid are given in column 5. The largest excursions are again at the poles, with 16.3 m height difference.

#### D. Higher-Order Bodies with Equator Symmetry

##### 1. Model 4a (Triaxial Ellipsoid)

In the preceding three ellipsoids, the longitude dependence of the geopotential has not been taken into account. For the present model, it is assumed that the geoid can be better approximated by a triaxial ellipsoid. How well it agrees with the geoid is one of the objectives of this investigation.

In a triaxial ellipsoid, the equator and all parallel sections exhibit a certain ellipticity, expressed -- in the geopotential -- by the sectorial coefficient  $J_{2,2}$ . The body is symmetrical with respect to the equator plane; hence, the odd-order terms in the spherical harmonics series of the geopotential (more exactly, of the radius vector of the surface) are zero. Thus, the earth is now assumed to be no longer symmetrical around the rotational axis.

The general formula of a triaxial ellipsoid is

$$\frac{x^2}{R_{e_0}^2} + \frac{y^2}{R_{e_1}^2} + \frac{z^2}{R_p^2} = 1, \quad (45)$$

where  $R_{e_0}$  and  $R_{e_1}$  are the two equatorial semi-axes. By introducing polar coordinates, Krause<sup>14</sup> has derived a general formula for the radius vector,

$$\frac{\bar{R}_e}{R} = \left[ \cos^2 \varnothing \frac{1 + \frac{1}{4} f_e^2 - f_e \cos 2(\lambda - \lambda_0)}{(1 - \frac{1}{4} f_e^2)^2} + \frac{\sin^2 \varnothing}{(1 - f)^2} \right]^{1/2}, \quad (46)$$

where  $\bar{R}_e$  is the mean equatorial radius, determined by the astrogeodetic and gravimetric methods of geodesy<sup>2,18</sup> and currently assumed to be<sup>1</sup>

$$\bar{R}_e = 6378165.0 \text{ m.}$$

The symbol  $\varnothing$  is the geocentric latitude of the parallel,  $\lambda$  is the longitude of the point on the surface, measured positive east of Greenwich,  $f$  is the meridional flattening of the ellipsoid,  $f_e$  is the ellipticity of the equator (and all parallel sections), and  $\lambda_0$  is the longitude of the apsidal line of the equatorial ellipse (i.e., the angle between the radius vector to the reference meridian on the equator and the semi-major axis of the equator ellipse, positive east of Greenwich), as well as the longitude of the associated parallel ellipses in both "hemispheres." Kaula<sup>6</sup> gives  $\lambda_0 = -14.5^\circ \pm 1.5^\circ$ . In reference 1, he quotes  $-8^\circ$  to  $-25^\circ$ ; however, more recent data indicate an improved value of<sup>14</sup>

$$\lambda_0 = -18^\circ \pm 3^\circ. \quad (47)$$

Thus, the semi-major axis of the equator ellipse is rotated by  $18^\circ$  west of the Greenwich meridian. Consequently, the largest equator radius is located approximately 600 st. miles north of Ascension Island in the Mid-Atlantic, and - diametrically opposed - in the vicinity of the Solomon Islands in the Pacific, while the shortest radii are approximately 500 st. miles south and west of Ceylon in the Indian Ocean and about 1800 st. miles west of Peru in the Pacific Ocean.

By solving Krause's radius equation (equation (15)) twice for  $\lambda = \lambda_0$  and  $\lambda = \lambda_0 \pm 90^\circ$ , respectively, at the equator ( $\varnothing = 0$ ) and introducing the derived expressions for  $R_{e_0}$  and  $R_{e_1}$  in the definition of the flattening (or oblateness),

$$f_e = \frac{R_{e_0} - R_{e_1}}{\bar{R}_e}, \quad (48)$$

one obtains a simple expression for the ellipticity of the equator, viz.,

$$f_e = 6 \cdot A_{2,2} = \frac{6}{\chi} J_{2,2}. \quad (49)$$

The best current value for  $J_{2,2}$  is given by Kaula<sup>6</sup>:

$$J_{2,2} = 1.8 \pm 0.1 \times 10^{-6}. \quad (50)$$

Using the most recent set of oblateness coefficients, equation (13), in the equation for the factor  $\chi$ , equation (22), one obtains

$$\chi = 0.9981691858. \quad (51)$$

With  $\chi$  and  $J_{2,2}$  (equation (50)), equation (49) yields

$$f_e = 10.81980906 \times 10^{-6} = 1 : 92423. \quad (52)$$

From equation (48) it is then found for the difference between the semi-major and semi-minor axis of the equator

$$\Delta R_e = R_{e_0} - R_{e_1} = 69.0 \text{ m}. \quad (53)$$

With the mean equatorial radius,  $\bar{R}_e$ , according to equation (35), the longest radius of the equator becomes

$$\bar{R}_e + \frac{\Delta \bar{R}_e}{2} = 6378199.5 \text{ m}$$

and the shortest radius

$$\bar{R}_e - \frac{\Delta\bar{R}_e}{2} = 6378130.5 \text{ m}$$

at the geographical locations described above.

The sectorial harmonic is depicted in figure 1.

The flattening  $f$  of the triaxial ellipsoid must be the same as for the "best" geoid (Model 5a and 5b) treated later, since the flattening equation, equation (58), contains only even zonal harmonics, in accordance with the symmetry behavior of the latter. With the even  $J_n$  of equation (13), equation (58) yields

$$f = 0.003353633015 = 1 : 298.184.$$

The polar radii then become

$$R_p = (1 - f) \bar{R}_e = 6378775.0 \text{ m.}$$

The surface of the triaxial ellipsoid has been computed for various latitudes and longitudes from equation (46). Results are given in table 4, column 2.

The gravity of the Model 4a ellipsoid can be determined from equation (26). All available even  $J_n$  are used, equation (13), with the odd zonal coefficients set equal to zero according to the assumed symmetry with respect to the equator plane. With  $\chi$  as given in equation (51), the factor  $\sigma$  becomes 0.9981683280, and the mean gravitation at the equator is then

$$\bar{g}_e = \sigma \frac{GM}{\bar{R}_e^2} = 978.0320 \text{ gal}$$

differing by 2 mgal from Kaula's Standard value.

Results are presented in table 4, column 5.

TABLE 4  
Models 4a and 4b

Longitude (deg)*		Radius of Tri-ellipsoid (m)	Radius of Symm. Spheroid (m)	Height of Spheroid (m)	Gravity of Spheroid (gal)
EOG	WOG				
LATITUDES 90N/90S (POLES)					
-		6356775.0	6356775.0	0	983.1815
LATITUDES 75N/75S					
0	180	6358203.0	6358203.0	0	982.8385
30	150	6358200.9	6358200.9	0	982.8376
60	120	6358199.0	6358199.0	0	982.8367
90	90	6358199.3	6358199.3	0	982.8368
120	60	6358201.4	6358201.4	0	982.8378
150	30	6358203.2	6358203.2	0	982.8386
LATITUDES 60N/60S					
0	180	6362109.2	6362114.2	4.9	981.9077
30	150	6362101.4	6362106.3	4.9	981.9041
60	120	6362094.5	6362099.3	4.8	981.9009
90	90	6362095.4	6362100.2	4.8	981.9013
120	60	6362103.2	6362108.1	4.9	981.9049
150	30	6362110.1	6362115.1	4.9	981.9081
LATITUDES 45N/45S					
0	180	6367456.9	6367461.7	4.7	980.6259
30	150	6367441.2	6367446.0	4.7	980.6186
60	120	6367427.4	6367432.0	4.6	980.6122
90	90	6367429.2	6367433.8	4.6	980.6131
120	60	6367444.8	6367449.6	4.7	980.6203
150	30	6367458.7	6367463.5	4.8	980.6267
LATITUDES 30N/30S					
0	180	6372818.1	6372819.3	1.1	979.3374
30	150	6372794.6	6372795.6	1.0	979.3263
60	120	6372773.7	6372774.7	1.0	979.3166
90	90	6372776.4	6372777.4	1.0	979.3179
120	60	6372800.0	6372801.0	1.0	979.3288
150	30	6372820.8	6372822.0	1.2	979.3384

\* EOG = East of Greenwich  
WOG = West of Greenwich

(Table 4 continued)

TABLE 4 (Continued)

Longitude (deg) EOG   WOG	Radius of Tri-Ellipsoid (m)	Radius of Symm. Spheroid (m)	Height of Spheroid (m)	Gravity of Spheroid (gal)
LATITUDES 15N/15S				
0 180	6376751.4	6376749.3	-2.1	978.3883
30 150	6376722.0	6376719.9	-2.1	978.3747
60 120	6376696.0	6376693.9	-2.1	978.3627
90 90	6376699.4	6376697.2	-2.2	978.3643
120 60	6376728.7	6376726.6	-2.1	978.3778
150 30	6376754.8	6376752.7	-2.1	978.3898
EQUATOR				
0 180	6378192.9	6378192.9	0	978.0448
30 150	6378161.4	6378161.4	0	978.0303
60 120	6378133.5	6378133.5	0	978.0175
90 90	6378137.1	6378137.1	0	978.0192
120 60	6378168.6	6378168.6	0	978.0337
150 30	6378196.5	6378196.5	0	978.0465

## 2. Model 4b (Symmetrical Geoid)

With the oblateness coefficients up to  $J_{14}$  readily available, it is of interest to investigate the deviation of the above triaxial ellipsoid from the surface of a quasi-ellipsoid, or rather "symmetrical geoid," derived from a series expansion of the known even zonal harmonics equivalent to the above employed gravity expansion. Using Krause's theory and solving equations (16) through (22), the coefficients in equation (15) are found to be

$$\begin{aligned}
 A_0 &= +0.9988800610 \\
 A_2 &= +0.2236730329 \times 10^{-2} \\
 A_4 &= -0.3180618021 \times 10^{-5} \\
 A_6 &= -0.6471848752 \times 10^{-6} \\
 A_8 &= -0.2704952265 \times 10^{-6} \\
 A_{10} &= -0.5409904530 \times 10^{-7} \\
 A_{12} &= -0.3576547995 \times 10^{-6} \\
 A_{14} &= +0.1793283168 \times 10^{-6}
 \end{aligned} \tag{54}$$

The surface equation, equation (15), then becomes

$$\begin{aligned}
 R_4 = & 6371021.84 - 14266.235 \cdot P_2(\sin \varnothing) + 20.29 \cdot P_4(\sin \varnothing) \\
 & - 4.13 \cdot P_6(\sin \varnothing) + 1.73 \cdot P_8(\sin \varnothing) + 0.345 \cdot P_{10}(\sin \varnothing) \\
 & + 2.28 \cdot P_{12}(\sin \varnothing) - 1.14 \cdot P_{14}(\sin \varnothing) + 34.51 \cdot \cos^2 \varnothing \\
 & \cdot \cos 2(\lambda + 18^\circ) \quad (\text{m}). \quad (55)
 \end{aligned}$$

Equation (55) has been computed for some values of  $\varnothing$  and  $\lambda$ ; results are given in column 3 of table 4. The deviation of the symmetrical geoid from the true triaxial ellipsoid is listed in the fourth column of table 4. Agreement is seen to be extremely good. Height differences are around 5 m in the higher latitudes. The largest height difference occurs around  $55^\circ$  North or South latitude, with over 6 m for all longitudes.

#### E. "Best" Geoid Bodies

##### 1. Model 5a ("Best" Geoid with Sectorial Term)

The most realistic model of the earth and its potential field must obviously make use of all available spherical harmonics coefficients, obtained from real-world observations. Using the theory developed recently by Krause<sup>13,14</sup>, it is -- as shown above -- relatively simple to express the geoid surface, assumed an equipotential level, in an expansion of spherical harmonics and appropriate coefficients. This "true" geoid is assumed as Model 5a of this investigation.

For the basic imposed constants (mean earth radius at equator, rate of the earth's rotation with respect to inertial space, and the gravitational parameter of the earth) the best currently available values<sup>1</sup> are chosen:

$$\begin{aligned}
 \bar{R}_e &= 6,378,165.0 \text{ m} \\
 \omega &= 0.729211585 \times 10^{-4} \text{ sec}^{-1} \\
 GM_{\oplus} &= 398603.2 \pm 3.0 \text{ km}^3 \text{ sec}^{-2}
 \end{aligned}$$

and for the additional parameters

$$J_{2,2} = 1.8 \pm 0.1 \times 10^{-6}$$

$$\lambda_0 = -18^\circ \pm 3^\circ.$$

Consistent with the above values, the mean equatorial gravitation is

$$\bar{g}_e = 978.0320 \text{ gal (see Model 4a).}$$

Solving again equations (16) through (22) for all available  $J_n$ , including odd orders, equation (13), the following  $A_n$ -coefficients of equation (15) are obtained:

$$\left. \begin{aligned} A_0 &= +0.9988800610 \\ A_1 &= 0 \\ A_2 &= +0.2236730329 \times 10^{-2} \\ A_3 &= -0.2550669802 \times 10^{-5} \\ A_4 &= -0.3180618021 \times 10^{-5} \\ A_5 &= -0.2103851762 \times 10^{-6} \\ A_6 &= +0.6471848752 \times 10^{-6} \\ A_7 &= -0.3336107793 \times 10^{-6} \\ A_8 &= -0.2704952265 \times 10^{-6} \\ A_9 &= -0.5309721113 \times 10^{-7} \\ A_{10} &= -0.5409904530 \times 10^{-7} \\ A_{11} &= +0.3025539200 \times 10^{-6} \\ A_{12} &= -0.3576547995 \times 10^{-6} \\ A_{13} &= -0.1142090956 \times 10^{-6} \\ A_{14} &= +0.1793283168 \times 10^{-6} \end{aligned} \right\} \quad (56)$$

with

$$\left. \begin{aligned} \chi &= 0.9981691858 \\ B_2 &= 0.3383437858 \times 10^{-2} \end{aligned} \right\}$$



The equation for the surface of the geoid becomes then\*:

$$\begin{aligned}
 R_S = & 6371021.844 - 14266.235 P_2(\sin \varnothing) + 16.268 P_3(\sin \varnothing) \\
 & + 20.286 P_4(\sin \varnothing) + 1.34 P_5(\sin \varnothing) - 4.127 P_6(\sin \varnothing) \\
 & + 2.127 P_7(\sin \varnothing) + 1.725 P_8(\sin \varnothing) + 0.338 P_9(\sin \varnothing) \\
 & + 0.345 P_{10}(\sin \varnothing) - 1.929 P_{11}(\sin \varnothing) + 2.28 P_{12}(\sin \varnothing) \\
 & + 0.728 P_{13}(\sin \varnothing) - 1.144 P_{14}(\sin \varnothing) + 34.505 \cos^2 \varnothing \cos 2(\lambda + 18^\circ),
 \end{aligned}
 \tag{m} \tag{57}$$

where  $P_n(\sin \varnothing)$  are the Legendre polynomials of argument  $\sin \varnothing^{**}$ .

By writing the radius equation, equation (15), for the poles ( $\varnothing = \pm 90^\circ$ ), one equation each results for the northern and the southern "hemispheres," which since

$$f = 1 - \frac{R_{pN} + R_{pS}}{2\bar{R}_e}$$

lead to an expression for the mean meridional oblateness of the geoid<sup>13,14</sup>

$$f = \frac{1}{X} \left\{ \sum_{\nu=1}^{\infty} \left[ 1 - (-1)^\nu \frac{1 \cdot 3 \cdot 5 \dots (2\nu - 1)}{2 \cdot 4 \cdot 6 \dots 2\nu} \right] J_{2\nu} + \frac{1}{2} \tilde{\omega}_e + B_2 \left( \frac{9}{2} J_2 - \tilde{\omega}_e - B_2 \right) \right\} \tag{58}$$

where  $X$  and  $B_2$  are given in equation (56) and  $\tilde{\omega}_e = 3461.414 \times 10^{-6} \text{ sec}^{-1}$ .

With Kozai's harmonics coefficients up to  $J_{14}$ , equation (58) yields

$$f = 0.003353633015 = 1 : 298.184,$$

---

\* Some of the amplitudes (coefficients) of the geoid-equation in reference 14 have been found to be slightly incorrect. The values are corrected here.

\*\* See Appendix A.

which is different from the currently accepted (Standard) value of 1960, viz.,

$$f = 1 : 298.30,$$

which is consistent with the old  $J_2$  (equation (37)) over a second-order Clairaut-type expression only, as mentioned earlier.

The surface of the "best" geoid, equation (57), and its gravity, equation (26), have been computed and are tabulated in table 5 for various latitudes and longitudes. It can be seen that the geoid, in accordance with the fact that of all tesseral harmonics only the first sectorial was included, is symmetrical around a plane defined by the major axis (at  $\lambda_0 = -18^\circ$ ) of the equator ellipse and the axis of rotation. If higher tesserals were taken into account, this last symmetry would also disappear.

The sectorial harmonic at the equator is shown in figure 1. The curve depicts (greatly exaggerated) the height of the "best" geoid over the rotationally symmetric geoid of Model 4b around the equator. At latitudes 45N and 45S, the amplitudes of the harmonic, for equal meridians, are half their value at the equator.

Because of the sectorial term depicted, the longest equator radius (also the longest radius vector to all latitudes) is at  $162^\circ\text{E}$  and at  $18^\circ\text{W}$  of Greenwich, with 6,378,199.5 m. The shortest radial vector is at  $72^\circ\text{E}$  and  $108^\circ\text{W}$  of the prime meridian, with 6,378,130.5 m. The difference amounts to 69.0 m.

At 45 degrees North and South parallel, the difference between the semi-major and semi-minor axis, as stated above, must be one-half of this value. It is 34.5 m.

At the poles, it is seen that the radial vector at the North Pole is longer than at the South Pole. The difference in height is 37.8 m, which accounts for the "pear" shape of the earth, suspected already in 1959 by O'Keefe<sup>8</sup>. The gravity at the North Pole is higher by 13.11 mgal than at the South Pole. Around the equator belt, the gravity varies by as much as 31.74 mgal (between the longitudes  $72^\circ$  and  $162^\circ\text{E}$ ). The mean equatorial gravity must be the same as for the triaxial ellipsoid, Model 4a; i.e.,

$$\bar{g}_e = 978.0320 \text{ gal.}$$

TABLE 5

## Geoid

Longitude*		Radius of Geoid (m)	Gravity of Geoid (gal)	Longitude*		Radius of Geoid (m)	Gravity of Geoid (gal)
EOG	WOG			EOG	WOG		
LATITUDE 90N (North Pole)							
-		6356793.9	983.18807				
LATITUDE 75N							
0	180	6358217.6	982.84373	90	90	6358213.8	982.84200
30	150	6358215.4	982.84275	120	60	6358215.9	982.84298
60	120	6358213.6	982.84189	150	30	6358217.8	982.84384
LATITUDE 60N							
0	180	6362118.1	981.90820	90	90	6362104.2	981.90178
30	150	6362110.3	981.90457	120	60	6362112.1	981.90540
60	120	6362103.3	981.90136	150	30	6362119.0	981.90861
LATITUDE 45N							
0	180	6367458.7	980.62507	90	90	6367430.8	980.61223
30	150	6367443.0	980.61782	120	60	6367446.6	980.61948
60	120	6367429.0	980.61140	150	30	6367460.5	980.62590
LATITUDE 30N							
0	180	6372812.7	979.33540	90	90	6372770.8	979.31614
30	150	6372789.0	979.32452	120	60	6372794.4	979.32701
60	120	6372768.1	979.31489	150	30	6372815.4	979.33664
LATITUDE 15N							
0	180	6376743.6	978.38634	90	90	6376691.6	978.36238
30	150	6376714.2	978.37281	120	60	6376721.0	978.37591
60	120	6376688.2	978.36083	150	30	6376747.0	978.38789

(table 5 continued)

\* EOG = East of Greenwich (degrees)  
WOG = West of Greenwich (degrees)

TABLE 5 (Continued)

Longitude EOG   WOG		Radius of Geoid (m)	Gravity of Geoid (gal)	Longitude EOG   WOG		Radius of Geoid (m)	Gravity of Geoid (gal)
LATITUDE 0 (EQUATOR)							
0	180	6378192.9	978.04484	90	90	6378137.1	978.01916
30	150	6378161.4	978.03034	120	60	6378168.6	978.03366
60	120	6378133.5	978.01750	150	30	6378196.5	978.04650
LATITUDE 15S							
0	180	6376755.0	978.39020	90	90	6376702.9	978.36623
30	150	6376725.6	978.37667	120	60	6376732.3	978.37976
60	120	6376699.6	978.36469	150	30	6376758.4	978.39174
LATITUDE 30S							
0	180	6372825.9	979.33889	90	90	6372784.0	979.31963
30	150	6372802.2	979.32801	120	60	6372807.7	979.33050
60	120	6372781.3	979.31838	150	30	6372828.6	979.34013
LATITUDE 45S							
0	180	6367464.7	980.62674	90	90	6367436.8	980.61390
30	150	6367448.9	980.61949	120	60	6367452.5	980.62115
60	120	6367435.0	980.61307	150	30	6367466.5	980.62757
LATITUDE 60S							
0	180	6362110.2	981.90722	90	90	6362096.3	981.90080
30	150	6362102.3	981.90360	120	60	6362104.1	981.90443
60	120	6362095.4	981.90039	150	30	6362111.1	981.90764
LATITUDE 75S							
0	180	6358188.5	982.83336	90	90	6358184.7	982.83164
30	150	6358186.3	982.83239	120	60	6358186.8	982.83261
60	120	6358184.5	982.83153	150	30	6358188.7	982.83347
LATITUDE 90S (South Pole)							
-		6356756.1	983.17496				

## 2. Model 5b ("Best" Geoid without Sectorial Term)

For purposes of comparison with models featuring circular equators, it is also of interest to determine the shape of the "best" geoid, with all available zonal harmonics coefficients, based on a circular equator. Model 5b is therefore obtained by solving equation (57) without the last (sectorial) term. Since the sectorial harmonic at the equator has already been determined in figure 1, the desired circular-equator shape is obtained by subtracting it from the radius vectors of Model 5a.

## IV. COMPARISON OF MODELS

In accordance with the different assumptions used, the various geographical theories to be compared here define geometrical bodies which differ from each other and from the geoid. Also, they lead to different gravity values for identical locations on the body. Primary attention is directed towards the deviations in geometries.

Figure 6 shows the radius vector as a function of latitude of Models 1, 2 and 3, referenced to the same body, i.e., the "best" geoid without the sectorial term (Model 5b). In all three cases, the bodies are not ellipsoids, but spheroids of revolution symmetrical around the equator plane, since they are based on superimposed spherical harmonics. It is seen that the widest deviation from the geoid is exhibited by Model 1, which takes into account solely the second order zonal harmonic,  $J_2$ . At the North Pole, the difference is -32.6 m; at the South Pole, +5.20 m. Since the spheroid of Model 1, as shown on table 1, differs from the Model 1 ellipsoid (flattening 1/298.254) by as much as -18.7 m at the North and South Pole, the deviation of the Model 1 ellipsoid from the reference geoid is less at the North Pole, amounting to -13.9 m, and higher (23.9 m) at the South Pole.

The spheroids of Models 2 and 3 are based on the old and the new set of coefficients  $J_2$ ,  $J_3$ ,  $J_4$ , respectively, as given by equations (39) and (44). In general, they agree very well with the reference geoid, exhibiting deviations of less than 5 m. At the poles, the deviation of the Model 2 spheroid from the reference line as well as from the improved Model 3 spheroid is larger, primarily due to the changes in  $J_2$  and  $J_3$ .

As in the case of Model 1, it is of interest to determine the deviation of the Model 2 spheroid from its associated ellipsoid, as given in table 2. The height of the spheroid based on the Standard values of  $J_2$ ,  $J_3$ ,  $J_4$  over the ellipsoid with consistent flattening 1/298.30 is shown in figure 7. Also plotted is the height of the "best" geoid without the  $J_{2,2}$ -term (Model 5b). The agreement between the two Model-2 bodies is good; the largest difference is at the South Pole, with 16.4 m. As is

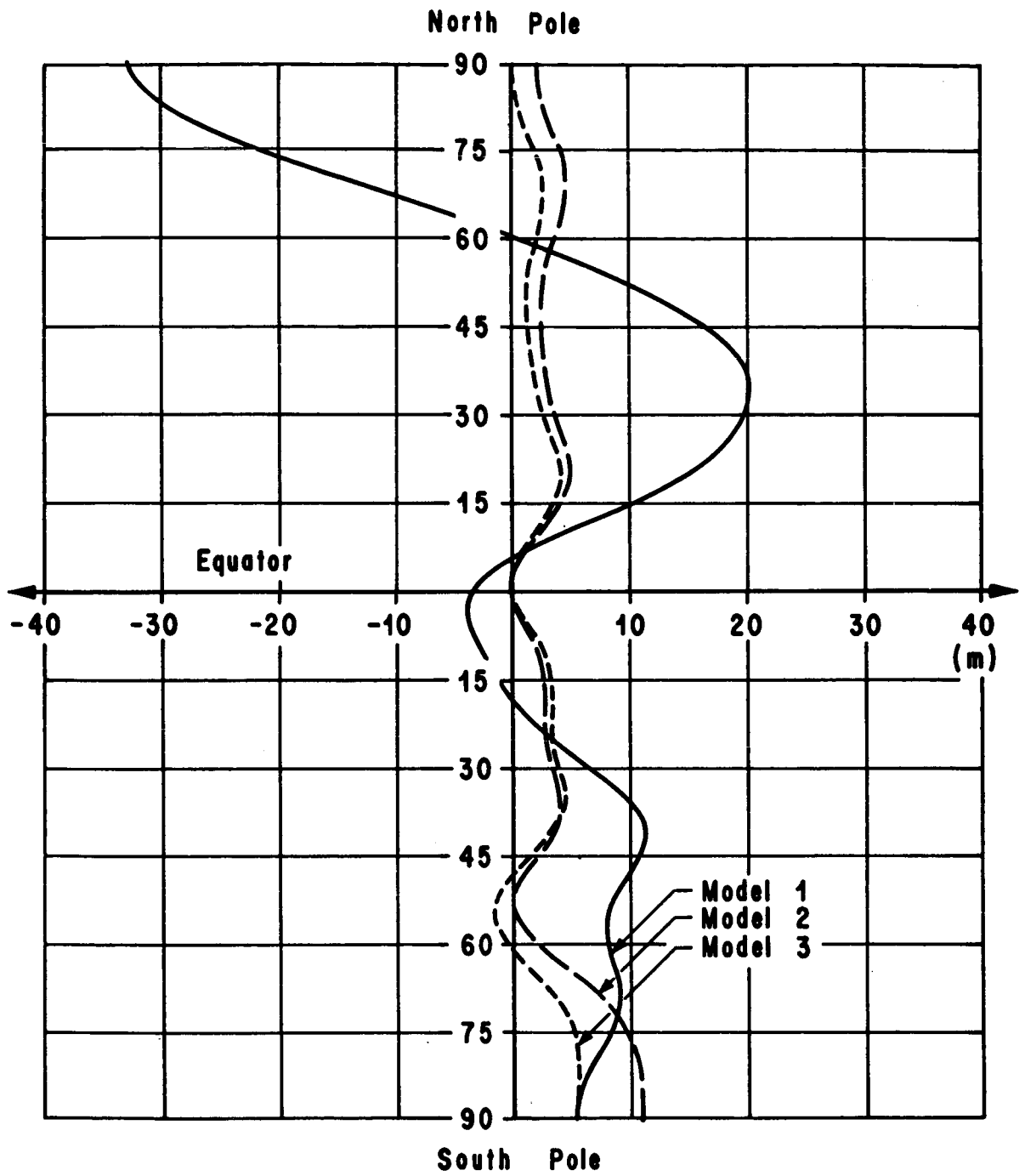


**FIG. 6. HEIGHT OF MODELS 1, 2 AND 3 (SPHEROIDS) OVER "BEST" GEOID WITHOUT SECTORIAL TERM**

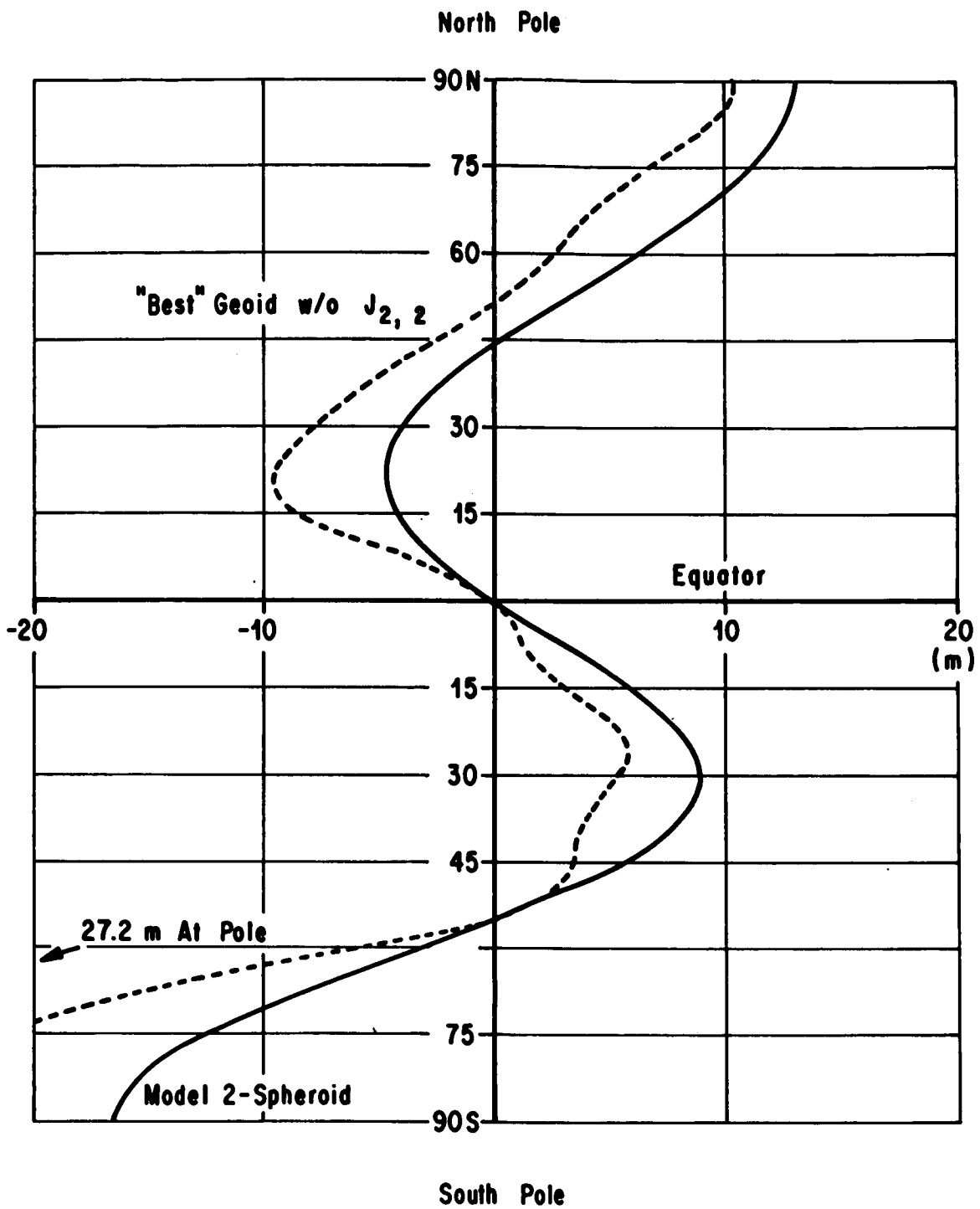


FIG. 7. HEIGHT OF MODEL 2-SPHEROID AND OF "BEST" GEOID WITHOUT SECTORIAL TERM, OVER STANDARD ELLIPSOID (1/298.3)

to be expected, the spheroid agrees better with the "best" geoid than the ellipsoid. The influence of particularly the odd zonal harmonics becomes manifest at the South Pole, where the Standard Ellipsoid, as used presently by NASA, deviates by as much as 27.2 m from the Model 5b-geoid.

A still better approximation to the "best" geoid with circular equator can be given with the spheroid of Model 3, as depicted in figure 8. Here, the spheroid height is referenced to the associated ellipsoid of flattening  $1/298.222$ , derived from the set of improved  $J_2$ ,  $J_3$ , and  $J_4$ . The deviations of the spheroid from the ellipsoid are numerically very similar to those between the Model 2 bodies, while the agreement of the ellipsoid with the circular-equator geoid has been improved considerably, except for the latitudes around 20N and 30S, where the gap is still almost 10 m. The agreement of the spheroid with the "best" geoid is generally better than 5 m.

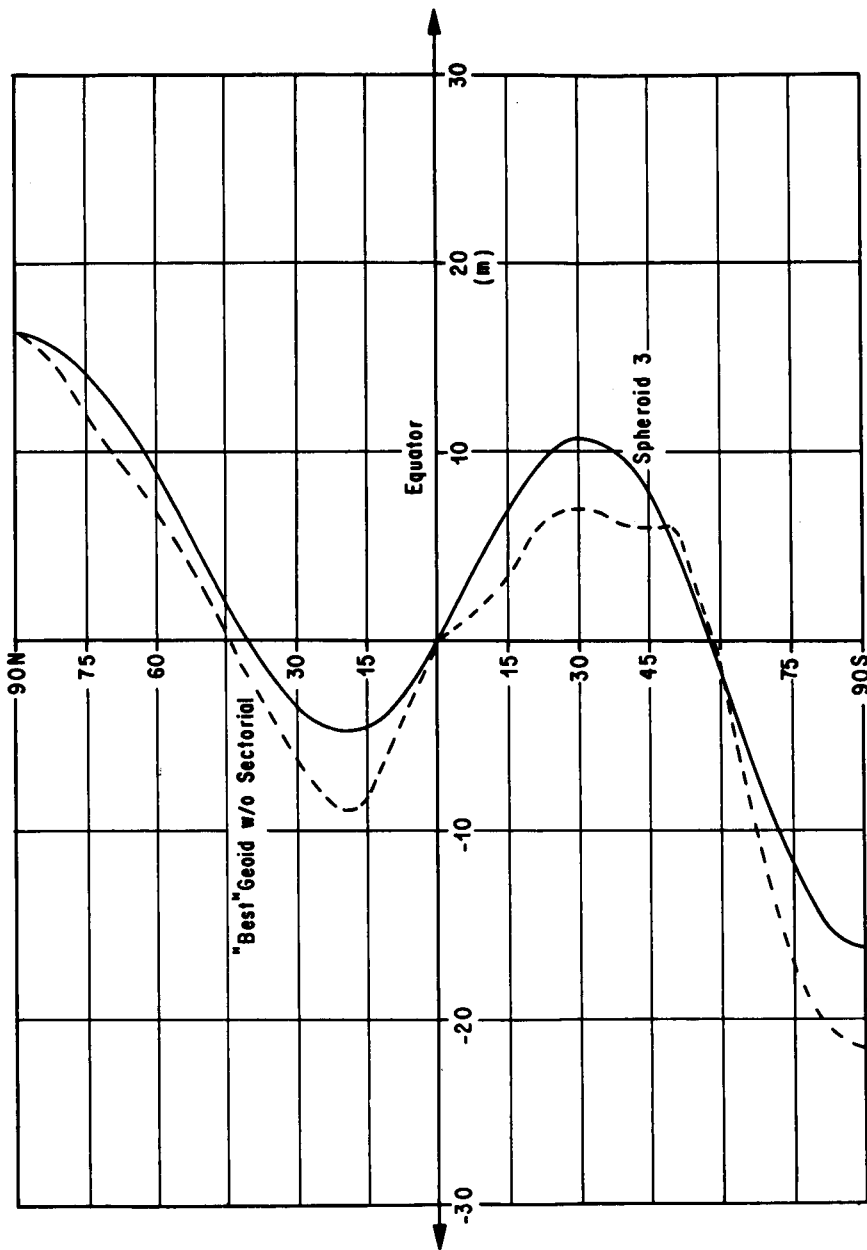
The height of the "best" geoid (Model 5a) has been computed from the data of tables 4 and 5, and is presented in figure 9 (greatly exaggerated), referenced to the triaxial ellipsoid of Model 4a. Both bodies are based on expansions of spherical harmonics up to and including  $J_{14}$ , with the latest available values for the coefficients. The sectional cut is along the prime meridian. The "pear" shape of the earth is clearly discernible. Since the mean equatorial radius is the same for both bodies (as well as the sectorial harmonic), they share the same equator. At the poles, however, deviations of the geoid are observable, amounting to 18.87 m at the North Pole, and to -18.87 m at the South Pole. In the intermediate latitudes, the deviations are less, with -8.5 m at 20 N and 7.7 m at 30S. The height differences are also plotted in figure 10, on a rectilinear grid, for a meridional section at Greenwich longitude.

According to the different harmonics coefficients used in the potential equation, the gravity of the analyzed models differs in each case. Using the gravitation of the "best" geoid (Model 5a) as tabulated in table 5, as common reference, the gravities of each model were computed for a meridional section along the prime meridian and plotted in figure 11. As is to be expected, the gravity of the triaxial ellipsoid (Model 4a), listed in table 4, agrees best (generally by better than  $\pm 3$  mgal) with the "best" geoid. The other models, with gravity values determined from differing values and numbers of oblateness coefficients, show generally identical behavior, with significant deviations (up to 35 mgal) at the poles and equator, in accordance with the recent findings of a more pronounced influence of the odd zonal harmonics, particularly  $J_3$ .

For Model 1, the exclusive use of  $J_2$  apparently compensates somewhat around the North Pole for the deviations in Models 2 and 3, which are obviously caused by the third order zonal harmonic, the only additional additive amplitude at these latitudes besides  $J_2$ . At the lower latitudes,



North Pole



South Pole

FIG. 8 HEIGHTS OF MODEL 3 - SPHEROID AND "BEST" GEOID WITHOUT SECTORIAL TERM OVER ELLIPSOID OF FLATTENING 1/298.222 (MODEL 3)

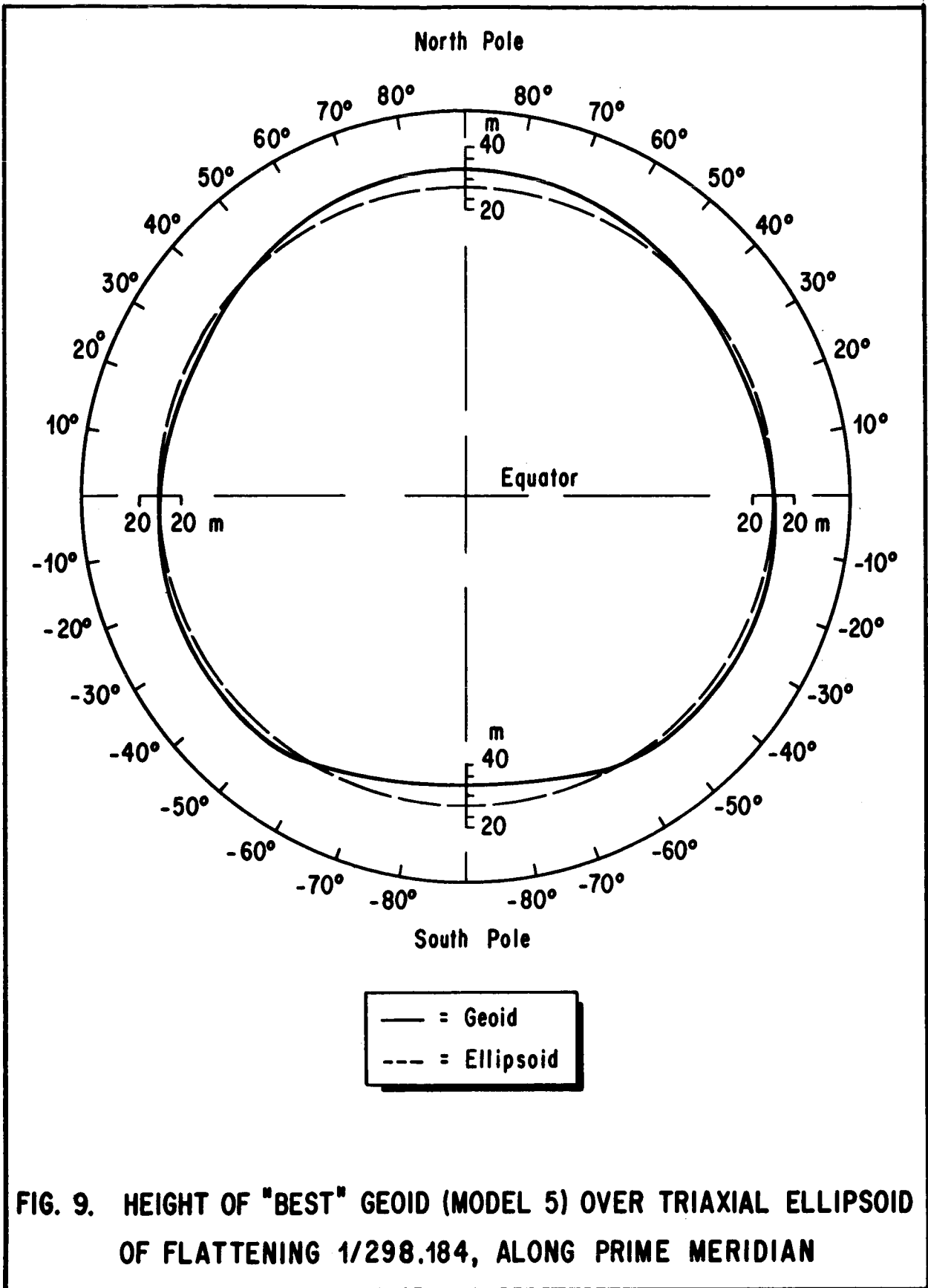


**FIG. 9. HEIGHT OF "BEST" GEOID (MODEL 5) OVER TRIAXIAL ELLIPSOID OF FLATTENING 1/298.184, ALONG PRIME MERIDIAN**

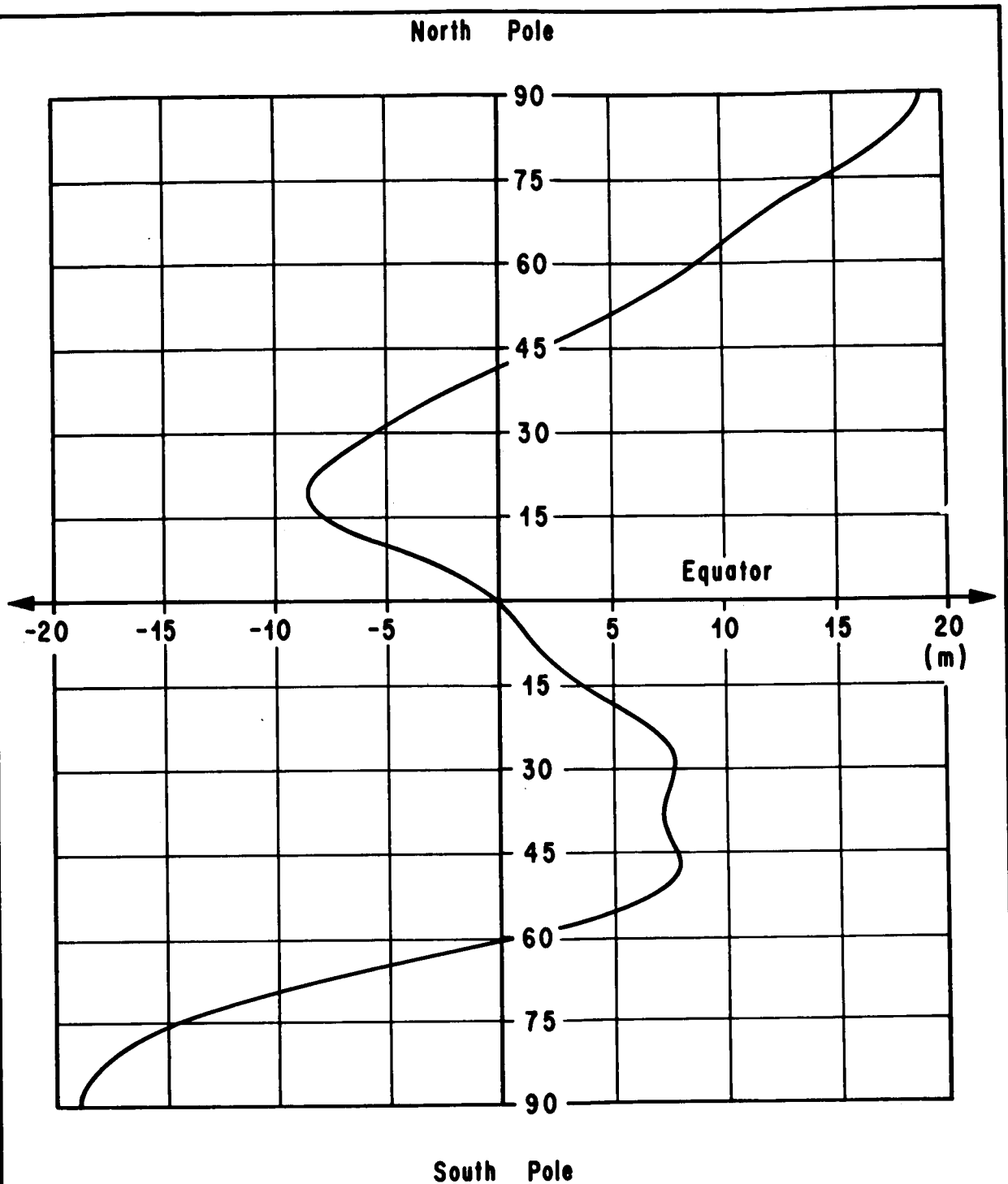


**FIG. 10. HEIGHT OF "BEST" GEOID (MODEL 5) OVER TRIAXIAL ELLIPSOID OF FLATTENING  $1/298.184$ , ALONG PRIME MERIDIAN**

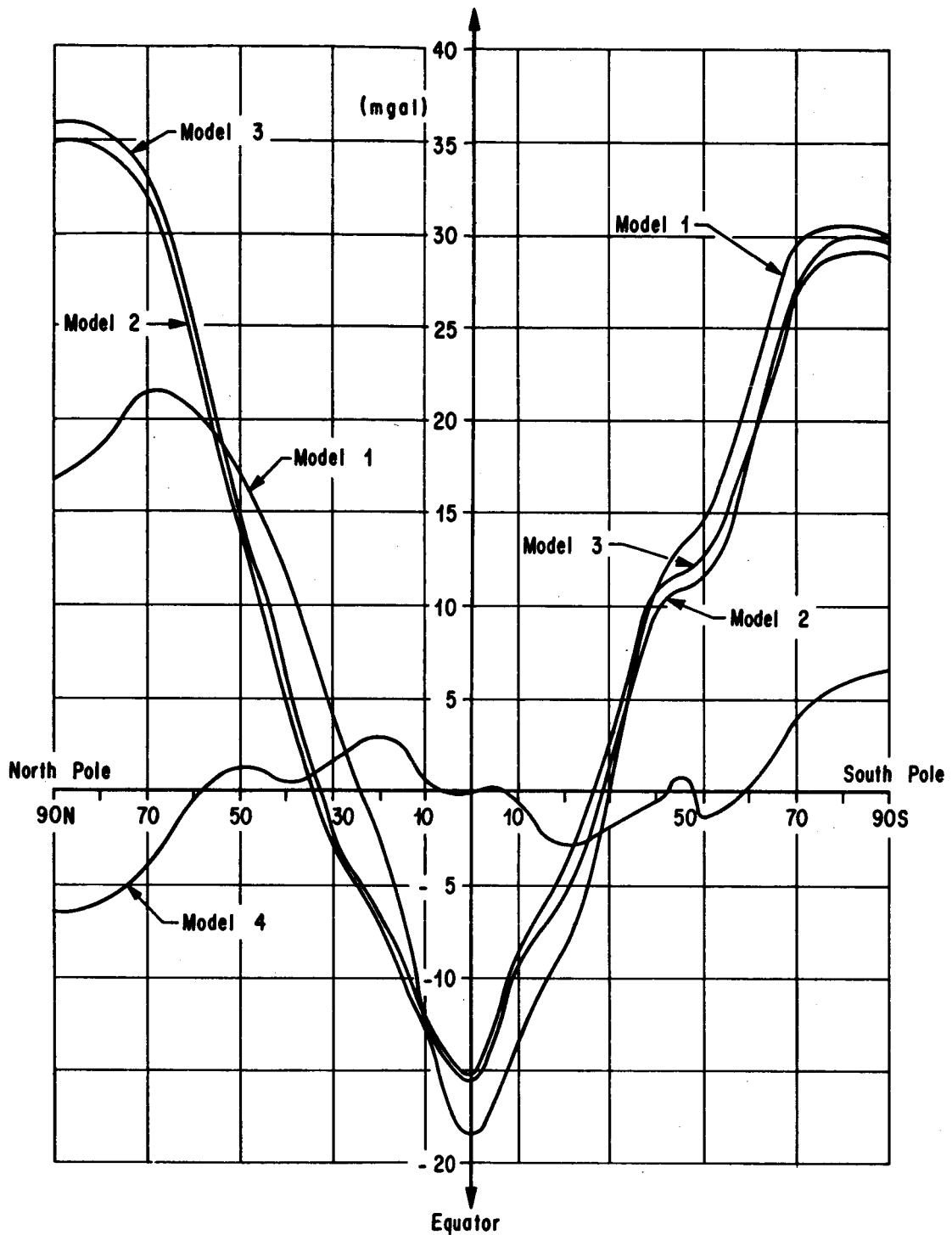


FIG. 11. DEVIATION OF GRAVITIES OF MODELS 1, 2, 3 AND 4 FROM GRAVITY OF "BEST" GEOID (MODEL 5), ALONG PRIME MERIDIAN

Model 3 -- with the improved set of coefficients -- agrees best of all three models with the reference, as is to be expected. However, the improvement is only very minor ( $< 1$  mgal), leading to the observation that the effects of improving the oblateness coefficients (rather than increasing their number beyond  $J_4$ ) are apparently revealed more significantly in the geometries than in the gravities of the bodies used.

## V. CONCLUSIONS

1. A new earth figure model, or geoid, has been developed<sup>13,14</sup> and computed here, consistent with the most recent oblateness coefficients available.

2. The currently used NASA Standard ellipsoid differs from this "best" geoid by -10.6 m at the North Pole, 9.6 m at  $20^\circ\text{N}$  parallel, -4.6 m at  $35^\circ\text{S}$  parallel, and as much as 27.2 m at the South Pole. If a spheroid based on a series expansion of spherical harmonics with the same oblateness coefficients as in the gravity equation were used instead, as provided by Krause's theory, these deviations could be reduced to 2.4 m, 4.9 m, 4.0 m, and 10.8 m, respectively. This surface formula would be more consistent with the gravity formulation.

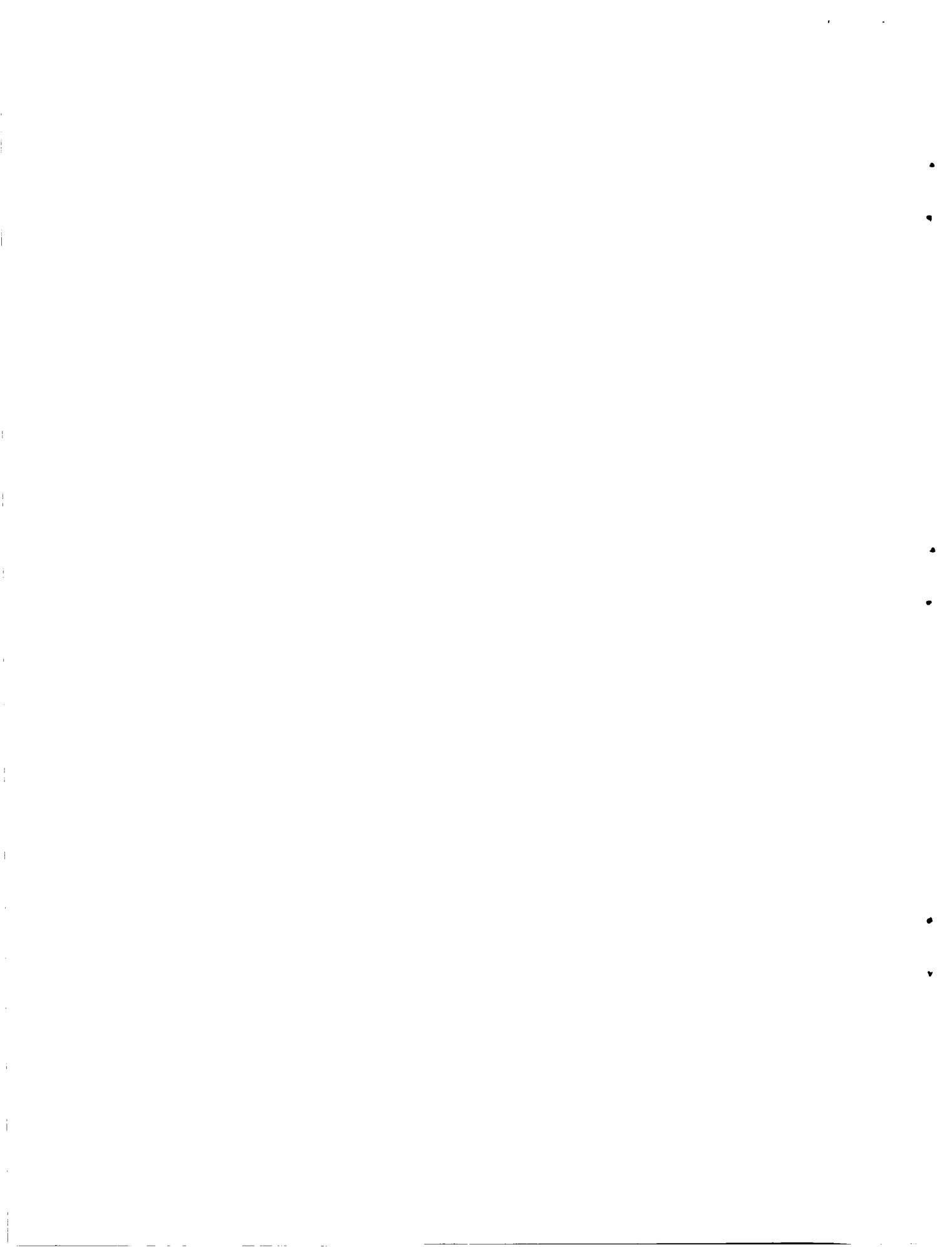
3. The currently used NASA Standard oblateness coefficients  $J_2$ ,  $J_3$ ,  $J_4$  result in gravity values, which differ from the gravity based on recent satellite measurements by as much as 35 mgal at the North Pole, -15.7 mgal at the equator, and 30 mgal at the South Pole (along the Meridian). Replacing the three J-coefficients by their updated values does not lead to significant improvements.

4. Conversely, updating the oblateness coefficients  $J_2$ ,  $J_3$ ,  $J_4$  in the NASA Standard geometry model (and using the series expansion, as noted above) could lead to significant improvements in height deviations (see figure 6), amounting to about 100 percent at the North Pole, 50 percent at the South Pole, and 30-50 percent at most of the intermediate latitudes.

5. For certain applications (e.g., guidance of short duration first-stage boosters), use of geographical and gravitational models based only on  $J_2$  may be permissible. Because of the shape of the  $J_2$ -harmonic (figure 2), it is advisable to use the ellipsoid (flattening  $1/298.254$ ), not the spheroid, as geometrical reference. Its height deviations from the "best" geoid (circular equator) are less than 10 m in the belt between  $65^\circ\text{N}$  and  $65^\circ\text{S}$  latitudes. The gravity of this simple model differs by maximally 30 mgal, at the South Pole (-18.5 mgal at equator, 16.8 mgal at  $90^\circ\text{N}$ ) from the sophisticated gravity model. The deviation is zero at about  $24^\circ\text{N}$  and  $30^\circ\text{S}$  parallels intersecting the Prime.

6. The latest available satellite measurements result in a "best" geoid which is pronouncedly "pear" shaped, with the north polar radius being 37.8 m longer than the south polar radius vector. The equator is slightly elliptic, with a difference of 69.0 m between the semi-major and semi-minor axes. The major axis of the equator ellipse is rotated West against the Prime Meridian. The rotation angle (longitude) is currently thought to be  $-18^\circ \pm 3^\circ$ . As shown by Krause, the "best" geoid can be described by a series expansion of spherical harmonics of the same degree as in the geopotential, the (amplitude) coefficients of which are directly related to the satellite-obtained oblateness coefficients.

7. As an approximation to the "best" geoid, an exact ellipsoid can be defined, as is customary in geodesy. The ellipsoid is a triaxial ellipsoid with the same equator ellipse as the geoid. The largest deviations of this body from the geoid are 18.87 m at the poles. In a band bounded by the parallels  $63^\circ\text{N}$  and  $70^\circ\text{S}$ , the height differences amount to less than 10 m. If for the geopotential of the triaxial ellipsoid only even J's are used, the gravity deviates from the geopotential of the geoid generally by less than 7 mgal and between  $70^\circ\text{N}$  and  $70^\circ\text{S}$  by less than 5 mgal.



## APPENDIX A

### Computation of Legendre Polynomials

The Legendre spherical functions  $P_n(x)$  are polynomials of the type

$$P_n(x) = \frac{1 \cdot 3 \cdot 5 \dots (2n-3)(2n-1)}{n!} \left[ x^n - \frac{n(n-1)}{2(2n-1)} x^{n-2} + \frac{n(n-1)(n-2)(n-3)}{2 \cdot 4(2n-1)(2n-3)} x^{n-4} - \dots \right]$$

$$n = 0, 1, 2, \dots$$

They are solutions of the differential equation

$$(1 - x^2) \frac{d^2y}{dx^2} - 2x \frac{dy}{dx} + n(n+1)y = 0.$$

For the present analyses, the Legendre functions were computed from the recurrence relation

$$(n+1)P_{n+1}(x) - (2n+1)xP_n(x) + nP_{n-1}(x) = 0,$$

where

$$x = \sin \vartheta$$

and starting with

$$P_0(\sin \vartheta) = 1$$

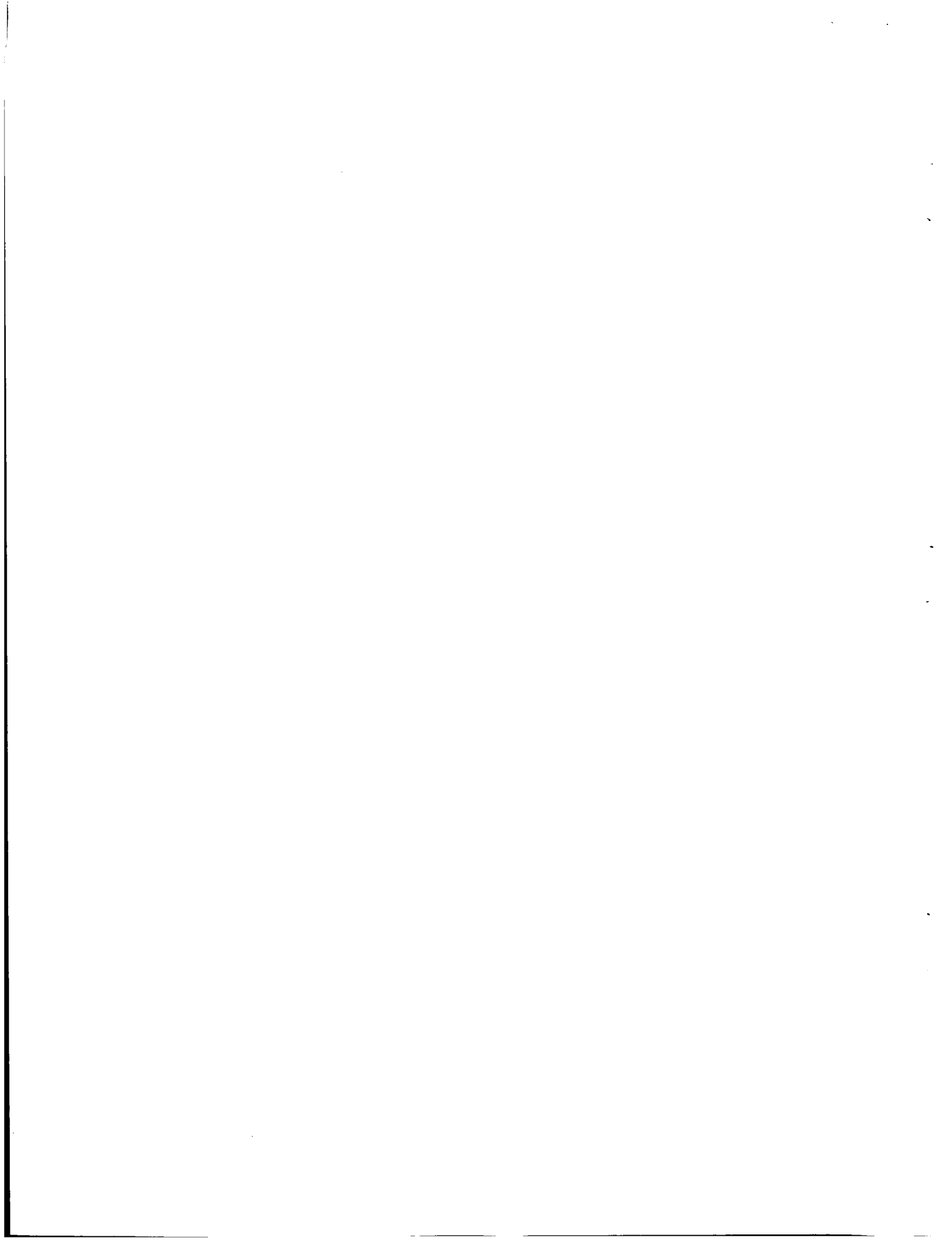
$$P_1(\sin \vartheta) = \sin \vartheta.$$

The most extensive tabulation of  $P_n(\cos \vartheta)$ , for  $n = 0(1)80$  and  $\vartheta = 0^\circ(1^\circ)180^\circ$ , has been published in reference 20. Since

$$\cos \vartheta = \sin(90^\circ \pm \vartheta),$$

the spherical functions can also be taken from this reference.





## APPENDIX B

### Alternate Expression for the Gravity Acceleration

Krause, in references 13 and 14, gives a form of the gravity,

$$\frac{g}{g_e} = C_0 - \sum_{n=1}^{\infty} (n+1) C_n P_n(\sin \varphi) + 3C_{2,2} \cos^2 \varphi \cos 2(\lambda - \lambda_0), \quad (59)$$

obtained from equation (26) by several transformations<sup>13</sup>. The coefficients  $C_n$  are related to the oblateness coefficients  $J_n$  and can be determined from them by relations similar to the equations (16) through (22) for the coefficients  $A_n$ , involving some of the latter.

$$C_0 = \frac{1}{X} \left[ 1 + 2(1 - A_0) - \frac{2}{3} \tilde{\omega}_e + \frac{1}{15} (3J_2 + \tilde{\omega}_e)^2 - \frac{1}{5} B_2(18J_2 + \tilde{\omega}_e - 3B_2) \right]$$

$$C_1 = 0$$

$$C_2 = \frac{1}{X} \left[ J_2 - \frac{2}{3} A_2 - \frac{2}{9} \tilde{\omega}_e - \frac{1}{63} (3J_2 + \tilde{\omega}_e)^2 + \frac{4}{21} B_2(18J_2 + \tilde{\omega}_e - 3B_2) \right]$$

$$C_4 = \frac{1}{X} \left[ J_4 - \frac{2}{5} A_4 + \frac{4}{175} (3J_2 + \tilde{\omega}_e)^2 + \frac{8}{175} B_2(18J_2 + \tilde{\omega}_e - 3B_2) \right]$$

$$C_K = \frac{1}{X} \left[ J_K - \frac{2A_K}{K+1} \right] \quad \text{for } K \neq 0, 2, 4$$

$$C_{2,2} = \frac{3}{X} J_{2,2}.$$

For the "best" geoid (Model 5a) with Kozai's set of  $J_n$  up to  $J_{14}$ , the C-coefficients become

$$\begin{aligned} C_0 &= 1.001760646 \\ C_1 &= 0 \\ C_2 &= -0.1172324264 \times 10^{-2} \end{aligned}$$

$$\begin{aligned}
C_3 &= -0.1272995717 \times 10^{-5} \\
C_4 &= +0.2636592115 \times 10^{-6} \\
C_5 &= -0.1401281566 \times 10^{-6} \\
C_6 &= +0.4619357542 \times 10^{-6} \\
C_7 &= -0.2500551096 \times 10^{-6} \\
C_8 &= -0.2102749240 \times 10^{-6} \\
C_9 &= -0.4245829102 \times 10^{-7} \\
C_{10} &= -0.4424481398 \times 10^{-7} \\
C_{11} &= +0.2520357773 \times 10^{-6} \\
C_{12} &= -0.3025300610 \times 10^{-6} \\
C_{13} &= -0.9786358495 \times 10^{-7} \\
C_{14} &= +0.1553740187 \times 10^{-6}.
\end{aligned}$$

With these coefficients, equation (59) then becomes\*, using  $g_e = 978.0320$ ,

$$\begin{aligned}
g &= 979753.968 + 3439.712 P_2(\sin \varnothing) + 4.980 P_3(\sin \varnothing) - 12.893 P_4(\sin \varnothing) \\
&+ 0.822 P_5(\sin \varnothing) - 3.163 P_6(\sin \varnothing) + 1.956 P_7(\sin \varnothing) \\
&+ 1.851 P_8(\sin \varnothing) + 0.415 P_9(\sin \varnothing) + 0.476 P_{10}(\sin \varnothing) \\
&- 2.958 P_{11}(\sin \varnothing) + 3.846 P_{12}(\sin \varnothing) + 1.340 P_{13}(\sin \varnothing) \\
&- 2.279 P_{14}(\sin \varnothing) + 15.873 \cos^2 \varnothing \cos 2(\lambda + 18^\circ) \quad (\text{mgal}). \quad (60)
\end{aligned}$$

With the Legendre polynomials obtained as shown in Appendix A, the gravitation can be computed for the "best" geoid from equation (60) as an alternative to the gravity equation (26).

---

\*Some of the amplitudes (coefficients) of the gravity equation in reference 14 have been found to be slightly incorrect. The values are corrected here.

## REFERENCES

1. Kaula, William M., "A Review of Geodetic Parameters," Paper X-640-63-55, International Astronomical Union Symposium No. 21, Paris, May 27-31, 1963. Also: NASA TN D-1847, May 1963.
2. Hopfner, Friedrich, Grundlagen der Höheren Geodäsie, Springer-Verlag, Wien, 1949.
3. Hagihara, Y., "Recommendations on Notation of the Earth Potential," *Astronom. J.* 67(1):108, February 1962.
4. King-Hele, D. G., G. E. Cook and Diana W. Scott, "Odd Zonal Harmonics in the Geopotential, Determined from Fourteen Well-Distributed Satellite Orbits," *Planet. Space Sci.* 1967, Vol. 15, pp. 741-769.
5. Sohn, R. L., "Trajectories for Unmanned Interplanetary Missions," Symposium on Unmanned Exploration of the Solar System, American Astronautical Society, Denver, Colo., February 8-10, 1965.
6. Kaula, William M., Theory of Satellite Geodesy, Blaisdell Publishing Co., Waltham, Mass.
7. Brouwer, D., "Solution of the Problem of Artificial Satellite Theory Without Drag," *Astronom. J.*, Vol. 64, p. 378, November 1959.
8. O'Keefe, J. A., A. Eckels and R. K. Squires, "Vanguard Measurements Give Pear-Shaped Component of Earth's Figure," *Science*, 129, 565-566, 1959.
9. King-Hele, D. G., G. E. Cook and Diana W. Scott, "The Odd Zonal Harmonics in the Earth's Gravitational Potential," *Planet. Space Sci.* 1965, Vol. 13, pp. 1212-1232.
10. Kozai, Yoshihide, The Use of Artificial Satellites for Geodesy, ed., G. Veis, 305-316.
11. Kozai, Yoshihide, "New Determination of Zonal Harmonics Coefficients of the Earth's Gravitational Potential," Smithsonian Inst. Astrophysical Observatory, Special Report No. 165, Cambridge, Mass., 1964.
12. King-Hele, D. G., G. E. Cook, and Diana W. Scott, "Even Zonal Harmonics in the Earth's Gravitational Potential: A Comparison of Recent Determinations," *Planet. Space Sci.* 1966, Vol. 14, pp. 49-52.

REFERENCES (Continued)

13. Krause, Helmut G. L., "Theory of a Refined Earth Figure Model," Paper presented at Symposium on Celestial Mechanics, Oberwolfach, West-Germany, Sept. 12-16, 1966.
14. Krause, Helmut G. L., "Theory of a Refined Earth Figure Model with Applications," paper presented at the Southeastern Symposium on Missiles and Aerospace Vehicles Sciences, American Astronautical Society, Huntsville, Ala., December 5-7, 1966.
15. Clarke, Victor C., Jr., "Constants and Related Data for Use in Trajectory Calculations," Jet Propulsion Laboratory Technical Report No. 32-604, March 1964.
16. Fischer, I., "An Astrogeodetic World Datum from Geoidal Heights Based on the Flattening  $f = 1/298.3$ ," J. Geophys. Res. 65(7):2067-2076, July 1960.
17. Kaula, William M., "A Geoid and World Geodetic System Based on a Combination of Gravimetric, Astrogeodetic, and Satellite Data," J. Geophys. Res. 66(6):1799-1811, June 1961.
18. Heiskanen, W. A. and F. A. Vening Meinesz, The Earth and Its Gravity Field, McGraw-Hill Book Co., Inc., New York, 1958.
19. Clausen, Th., Astronomische Nachrichten, Vol. 18, No. 418, p. 145, 1841.
20. Clark, G. C. and Stuart W. Churchill, Tables of Legendre Polynomials, Engineering Research Inst., University of Michigan, 1957.

## SURVEY AND COMPARATIVE ANALYSIS OF CURRENT GEOPHYSICAL MODELS

by Jesco von Puttkamer

The information in this report has been reviewed for security classification. Review of any information concerning Department of Defense or Atomic Energy Commission programs has been made by the MSFC Security Classification Officer. This report, in its entirety, has been determined to be unclassified.

This document has also been reviewed and approved for technical accuracy.



---

E. D. Geissler  
Director, Aero-Astroynamics Laboratory

## DISTRIBUTION

NASA TM X-53677

DIR

Dr. von Braun

DEP-TDr. Rees  
Mr. NeubertR-DIR

Mr. Weidner

R-P&VEDr. Lucas  
Mr. GoernerR-ASTR

Dr. Haeussermann (3)

R-COMP

Dr. Hoelzer

R-SSLDr. Stuhlinger  
Mr. Heller  
Dr. HaleR-ASMr. Williams  
Mr. Becker  
Mr. Fellenz

MS-T (6)

MS-IP

MS-IL (8)

MS-H

CC-P

I-RM-M

R-AERODr. Geissler  
Mr. Jean  
Dr. H. Krause  
Dr. Heybey  
Mr. Cummings  
Mr. Mabry  
Mr. Nathan  
Mr. Few  
Mr. von Puttkamer (50)  
Mr. Horn  
Dr. McDonough  
Mr. Baker  
Mr. Dahm  
Mr. Lindberg  
Mr. Vaughan  
Mr. T. Deaton  
Mr. Cremin  
Mr. Toelle  
Mr. Lester  
Mr. Gillis  
Mrs. Chandler  
Mr. Rheinfurth  
Mr. Ryan  
Mr. R. Smith  
Mr. O. Vaughan  
Mr. O. Smith  
Mr. Kaufman  
Mr. Hagood  
Mr. Hardage  
Mr. Hill  
Mr. Thomae  
Mr. Scott  
Mr. Ellison  
Mr. Young  
Mr. Wheeler  
Mr. Goldsby  
Mr. Blair  
Mr. Causey  
Mr. Schwaniger  
Dr. Festa

EXTERNAL DISTRIBUTION

Office of Manned Space Flight  
NASA Headquarters  
Washington, D. C. 20546

Office of Space Science and Application  
NASA Headquarters  
Washington, D. C. 20546

Office of Advanced Research and Technology  
NASA Headquarters  
Washington, D. C. 20546

NASA-Langley Research Center  
Hampton, Va. 23365  
Attn: Library (5)

NASA-Manned Spacecraft Center  
Houston, Texas 77001  
Attn: Library (5)

NASA-Ames Research Center  
Moffett Field, Mountain View, Calif. 94035  
Attn: Library (5)

NASA-Goddard Space Flight Center  
Greenbelt, Maryland 20771  
Attn: Library (5)

Jet Propulsion Lab.  
Calif. Inst. of Tech.  
4800 Oak Grove Dr.  
Pasadena 3, California 91103  
Attn: Library (5)

NIKE-X Project Office  
U. S. Army  
Redstone Arsenal, Ala.  
Attn: Dr. Oswald Lange

Army Missile Command  
Redstone Arsenal, Alabama  
Attn: Library (5)

NASA-John F. Kennedy Space Center  
Kennedy Space Center, Fla. 32899  
Attn: Dr. Knothe (2)  
Library (5)

Sci. & Tech. Info. Facility (25)  
Attn: NASA Rep. (S-AK/RKT)  
P. O. Box 33  
College Park, Md. 20740